NASA/CR—2001-210706

Jet Plume Flow Solutions

Percy J. Bobbitt
Eagle Aeronautics, Inc., Newport News, Virginia

K.S. Abdol-Hamid
Analytical Services and Materials, Inc., Hampton, Virginia

Armin Wulf
ICEM CFD Engineering, Inc., Berkeley, California

Ana F. Tinetti
Eagle Aeronautics, Inc., Newport News, Virginia

May 2001

The NASA STI Program Office . . . in Profile

Since its founding, NASA has been dedicated to the advancement of aeronautics and space science. The NASA Scientific and Technical Information (STI) Program Office plays a key part in helping NASA maintain this important role.

The NASA STI Program Office is operated by Langley Research Center, the Lead Center for NASA's scientific and technical information. The NASA STI Program Office provides access to the NASA STI Database, the largest collection of aeronautical and space science STI in the world. The Program Office is also NASA's institutional mechanism for disseminating the results of its research and development activities. These results are published by NASA in the NASA STI Report Series, which includes the following report types:

- TECHNICAL PUBLICATION. Reports of completed research or a major significant phase of research that present the results of NASA programs and include extensive data or theoretical analysis. Includes compilations of significant scientific and technical data and information deemed to be of continuing reference value. NASA's counterpart of peer-reviewed formal professional papers but has less stringent limitations on manuscript length and extent of graphic presentations.

- TECHNICAL MEMORANDUM. Scientific and technical findings that are preliminary or of specialized interest, e.g., quick release reports, working papers, and bibliographies that contain minimal annotation. Does not contain extensive analysis.

- CONTRACTOR REPORT. Scientific and technical findings by NASA-sponsored contractors and grantees.

- CONFERENCE PUBLICATION. Collected papers from scientific and technical conferences, symposia, seminars, or other meetings sponsored or cosponsored by NASA.

- SPECIAL PUBLICATION. Scientific, technical, or historical information from NASA programs, projects, and missions, often concerned with subjects having substantial public interest.

- TECHNICAL TRANSLATION. English-language translations of foreign scientific and technical material pertinent to NASA's mission.

Specialized services that complement the STI Program Office's diverse offerings include creating custom thesauri, building customized data bases, organizing and publishing research results . . . even providing videos.

For more information about the NASA STI Program Office, see the following:

- Access the NASA STI Program Home Page at ***http://www.sti.nasa.gov***

- E-mail your question via the Internet to help@sti.nasa.gov

- Fax your question to the NASA Access Help Desk at 301–621–0134

- Telephone the NASA Access Help Desk at 301–621–0390

- Write to:
  NASA Access Help Desk
  NASA Center for AeroSpace Information
  7121 Standard Drive
  Hanover, MD 21076

NASA/CR—2001-210706

Jet Plume Flow Solutions

Percy J. Bobbitt
Eagle Aeronautics, Inc., Newport News, Virginia

K.S. Abdol-Hamid
Analytical Services and Materials, Inc., Hampton, Virginia

Armin Wulf
ICEM CFD Engineering, Inc., Berkeley, California

Ana F. Tinetti
Eagle Aeronautics, Inc., Newport News, Virginia

Prepared under Contract C73174-J

National Aeronautics and
Space Administration

Glenn Research Center

May 2001

Available from

NASA Center for Aerospace Information
7121 Standard Drive
Hanover, MD 21076

Available electronically at http://gltrs.grc.nasa.gov/GLTRS

PREFACE

In 1995, NASA GRC initiated efforts to meet the US industry's rising need to develop jet noise technology for separate flow nozzle exhaust systems. Such technology would be applicable to long-range aircraft using medium to high by-pass ratio engines. With support from the Advanced Subsonic Technology Noise Reduction program, these efforts resulted in the formulation of an experimental study, the Separate Flow Nozzle Test (SFNT). SFNT's objectives were to develop a data base on various by-pass ratio nozzles, screen quietest configurations and acquire pertinent data for predicting the plume behavior and ultimately its corresponding jet noise. The SFNT was a team effort between NASA GRC's various divisions, NASA Langley, General Electric, Pratt&Whitney, United Technologies Research Corporation, Allison Engine Company, Boeing, ASE FluiDyne, MicroCraft, Eagle Aeronautics and Combustion Research and Flow Technology Incorporated.

SFNT found several exhaust systems providing over 2.5 EPNdB reduction at take-off with less than 0.5% thrust loss at cruise with simulated flight speed of 0.8 Mach. Please see the following SFNT related reports: Saiyed, et al. (NASA/TM—2000-209948), Saiyed, et al. (NASA/CP—2000-210524), Low, et al. (NASA/CR—2000-210040), Janardan et al. (NASA/CR—2000-210039), Bobbitt, et al. (NASA/CR—201-210706) and Kenzakowski et al. (NASA/CR—2001-210611.).

I wish to thank the entire SFNT team of nearly 50 scientists, engineers, technicians and programmers involved in this project. SFNT would have fallen well short of its goals without their untiring support, dedication to developing the jet noise technology.

Naseem Saiyed
SFNT Research Engineer

INTRODUCTION

The use of mixers and mufflers on jet engine exhausts for noise reduction has been a subject of investigation for a number of years. As noise restrictions become more severe and human tolerance is diminished, the search for better mixers and/or mufflers continues. This report details the result of one such study in which a concept for fan and core-flow mixing is analytically investigated. This concept, like many other bypass schemes, is intended to promote the mixing of the hot and energetic core flow with the cold fan flow. The noise reduction that ensues must be evaluated as well as the associated performance penalty. Calculations are carried out using the Navier-Stokes equations and appropriate turbulence models.

To perform the required study Eagle Aeronautics, Inc., (EAI) has put together a team that is composed of EAI, Analytical Service and Materials (AS&M) and ICEM CFD Technologies (ICEM). Each possesses extensive experience in the technologies that constitute computational fluid dynamics (CFD). Expedition of the subject contract has required each group to contribute in areas where they have a particular, or unique, knowledge. The composite of these inputs yields a very accurate and time-efficient methodology/code-array for use in a variety of nozzle applications. One nozzle configuration in the present study is axisymmetric and two others are three dimensional due to the geometry of the "mixing" device. The 3D configurations are periodic in the cross plane; only one section of a configuration is analyzed with periodic boundary conditions applied for flow conditions at zero angle of attack.

The basic flow solver of the Navier-Stokes equations is PAB3D, which was developed by Dr. Khaled S. Abdol-Hamid of AS&M under contract to the NASA Langley Research Center. Dr. Armin Wulf of ICEM using their COMAK generated surface and field grids and Hexa codes. Post processing was done by Ms. Ana Tinetti using the POST code developed by Dr. Steven Massey, both of EAI.

In the present report a brief discussion of the nozzle geometries, grid methodology, the flow solver, and the calculated results obtained are given in that order. Computation times, which are of particular concern for the 2D and 3D configurations, are also noted.

METHODOLOGY

Nozzle Geometries

Both axisymmetric and three-dimensional nozzles are analyzed in this study. The 3D nozzles are similar to the axisymmetric except for 12 or 24 tabs (or chevrons) arrayed around the trailing edge of the core nozzle. They are alternately deflected inward and outward with respect to the baseline axisymmetric nozzle geometry. Figure 1 shows a cross-section of the 2D nozzle while figure 2 shows the geometry of the modified core nozzle of the $3A_{12}B$, GE configuration. Figure 3 gives a photograph of this same nozzle showing more clearly the core-nozzle tabs.

The Eagle team added a second 3D nozzle to illustrate the rapidity that geometry perturbations could be made. It is designated $3A_{24}B$ since it has twice as many tabs as the $3A_{12}B$ nozzle.

Grid Generation

The most time consuming job in applying CFD Navier-Stokes and Euler codes is the creation of the surface and field grids. Starting with a given geometry informed decisions with respect to the blocking structure and the grid resolution must be made. One must also estimate where large flow gradients are expected and concentrate more grid points in these areas to accurately resolve them. Solutions using the initial grid system will usually turn up regions where the grid will need further refinement or where fewer points can be used. Areas of high grid skewness and aspect ratio must be corrected; grid equivalency between various blocks should be checked. It is extremely important in CFD to generate a grid that takes into account all of the geometric and flow characteristics of the problem at hand as well as the stability of the solution methodology.

Surface modeling and grid generation in the present study was the responsibility of ICEM and was expedited using their CFD COMAK and CFD Hexa codes. The latter has unique automatic features enabling efficient (fast) geometry perturbations as indicated in the list below.

- Rapid block structure initialization.
- Easy-to-use tools allowing the user to detail the initial block structure (block splitting, adjustment to given geometry, etc.).
- Automatic insertion of O-grid topologies in the block structure (excellent discretization of near surface regions, enormous time saver compared to conventional systems).
- Automated set up of structured bunching based on a minimum of user input.
- Fully automatic meshing of the block structure (e.g., nodes associated to geometry surfaces are projected onto these surfaces).
- Periodic grids.
- H-grid refinement (hanging nodes).
- Sub-topologies to easily handle repetitive components or sub-configurations in large configurations.
- Replay Mode: automated parametric meshing of similar geometries.

In this project, a 2D parametric geometry model and grid and a 3D parametric geometry model and grid were developed for the nozzles shown in figures 1 and 2. The input convention for the geometry is shown in figure 4. The user simply provides a file with 12 named curves: 7 horizontally oriented curves named C1, C2, C3, C41, C42, C51 C52 and CSYM for the curve representing the center axis and 4 vertically oriented curves CV1, CV2, CV3 and CV4. The file with the curves needs to be called INPUT_P and needs to be provided as a Object part for Comak in the ICEM CFD manager. All curves need to be NURB curves. The walls near the core-nozzle trailing edge will be collapsed in the program. In addition, the user needs to provide a set of parameters that dictate where the nozzle wall thickness goes to zero. For the 2D case, the parameters are denoted as K-R1, K-R2, K-OP and K-OP2 as given in figure 5. The blocking structure is shown in figure 6 and the numbering scheme for the 8-block grid in figure 7.

Figure 8 shows the "initial cut" of the 2D grid in and just downstream of, the 2D nozzle (also see figure 6). Subsequently, several iterations were required to reconfigure the downstream grid with the aid of PAB3D solutions, in order to better define the shear layers between the core and

fan flows and between the fan and free-stream flows. Figures 9 and 10 show the result of this exercise including the new K parameter values (figure 9) and the final near-field and internal grid (figure 10). A total of 189,400 grid points were utilized.

Except for the region on and above the tabs, the 3D grid is the same as the 2D. In the 3D case, the user needs to provide four more curves in the Object part. The curves are the inner edge curves of the first two tabs (½, 1, ½) T1, T2, T3 and T4 as defined in figure 11. In addition, an opening angle K-PE must be defined. These angles, along with the appropriate K values, are given in figure 12. The outer core nozzle wall will be collapsed at the leading edge of the tabs in the program, i.e., the tabs are considered as thin sheet metal. All subsequent steps are automated and an input file for PAB3D is generated. The generation of the 3D parametric surface model takes about 5 minutes on an SGI Octane and the 3D parametric volume grid, with 2.49 million cells, takes about 4 minutes. Additional details of the grid-generation methodology are given in Appendix A.

The automatically generated 3D surface model for the nozzle with 12 tabs is shown in figure 13a along with the surface grid for a 30 degree section (required for PAB3D) in figure 13b. Figure 14 shows the 9-block structure of the final 3D grid. Near field as well as the entire-field grids are shown in figures 15 and 16. A total of 2,492,677 grid points were utilized.

A 24 tab grid was required for our 24 tab, core nozzle configuration and is similar to that for the 12 tab except only a 15 degree sector is required due to the reduced size of the tabs. This new grid took less than 9 minutes to construct on an SGI Octane.

PAB3D Navier-Stokes Solver

The PAB3D flow solver is widely used in the United States aerospace industry for propulsion component design, aircraft system analysis, and environmental quality studies including jet engine acoustics. The solution methodology embodied in the PAB3D code can be applied to a much wider range of problems for general industry and academia as a research tool or a teaching aid.

The PAB3D code uses the Roe scheme to approximate the inviscid terms. The inviscid terms in the Navier-Stokes equations in the Roe scheme are cast in the form of an approximate Riemann problem. The interface flux in the streamwise direction is determined by separate terms, depending on the quantities on the left (upstream) and the right (downstream) sides of the interface. The downstream term is a significant part of any elliptic problem, has a value of zero for hyperbolic or supersonic problem and can be ignored without introducing a significant flow solution for parabolic problems. By ignoring the downstream dependence terms in the Roe scheme, the solver becomes the space-marching scheme. Under the modified scheme, a solution is obtained plane by plane from upstream to downstream by carrying out a sufficient number of implicit iterations in each plane. A solution for the entire computational domain is established in a single sweep. When the space-marching option is used for jet flow computations as conditions permit, the computer time is less than one-twentieth of the time

required for obtaining a time marching solution with the same flow condition. The accuracy obtained by these different solvers is practically indistinguishable.

PAB-3D has other built-in timesaving routines including grid sequencing and customized computer memory requirements that permit the user to quickly obtain a converged solution. PAB3D uses advanced turbulent models to model the Reynolds Stress terms in the governing equations. There are several state-of-the-art two-equation and algebraic Reynolds Stress turbulence models implemented in the PAB3D code. PAB3D is also capable of simulating different gases (species) simultaneously for real gas simulations. The species concentrations are used to evaluate equivalent thermodynamic and viscous parameters in the flow governing equations. All scalar equations (turbulence and species concentration) are solved uncoupled from the mean flow governing equations. This approach keeps the scheme partially implicit with a reduction in computational time.

PAB3D uses either natural or specified locations for the transition of the flow from laminar to turbulent. Turbulent calculations do not require any special initialization procedure for stable computation. The code uses a flexible mesh sequencing procedure. Typical solutions will require 800 iterations on a twice-coarsened mesh level, 400 iterations on a one-coarsened mesh level, and 200 iterations on the finest mesh level. For example, 1,000,000 grid points require 25-30 hours using an SGI R10000/185 MHz workstation.

Another approach to reducing computation time is to use distributed computers or a multiprocessor computer. GEAE has recently used the MPI (Message Passing Interval) version of PAB3D to produce a solution for an equivalent nozzle-exhaust problem with CHEVRON (noise suppression device). They used six HP 9000 computers and got a converged solution in approximately 12 hours. Calculations for the 3D nozzle configurations in this study were carried out using a cluster of four CPU SGI R 10000/195 MHz computers (roughly equivalent to three Dec alpha 21164/533 MHz computers) and the MPI version of PAB3D. Appendix B gives a detailed description of the virtues of computer clusters versus a single C-90 processor.

Three major grid divisions were created in the grid generation to reduce computational time. The nozzle section was first run alone using a static backpressure boundary condition and an elliptic solution procedure. The external nozzle section was run with the same approach. The downstream section was run using the inflow from the nozzle and external nozzle sections in a parabolic mode to provide an initial estimate of the flow solution. The initial estimate was used to adapt the grid (as noted earlier) before continuing. The three-grid sections were combined and run elliptically to provide the final solution including the interaction of the internal and external flows. The combined grid, up to 3 million grid points, will fit in the 300 MB of memory on a workstation. The solution strategy is summarized below.

- Y+ is around 1 for the fine grid, and designed for not to exceed a value of 6 at the coarser grid level. This makes the coarse and medium grid simulation accurate less than 5 percent but represents quantitatively most of the flow characteristics.
- 4 CPU SGI R10000/195 MHz system is used to simulate the 3D cases, with speed equivalent to 3 CPU Alpha 21164/533 MHz.

- Use the coarse grid level to define the elliptic and parabolic region, which is 1/64 of the fine grid.
- Use the time marching and grid sequencing technique to simulate the elliptic flow region.
- Use the space marching to simulate the parabolic region.

The PAB3D code has been used to provide solutions for each condition using the following options in the PAB3D code.

- Mixed Roe/van Leer scheme: Roe's scheme for the internal region of the nozzle and van Leer's for the jet mixing layer region. This mix will provide the best combination based on our experience.
- Both time-marching and space-marching schemes will be used for faster converged solutions. Typical 1,000,000 grid points require less than 6 hours for converged solution.
- Third-order accuracy in space.
- Multiblock structured with general conservative patching technique.
- Standard two equation k-_ model.
- Shih, Zhu and Lumley Algebraic stress model.

A two-equation eddy-viscosity model and a non-linear algebraic Reynolds stress (SZL) model solution will be provided for the 12 tab 3D configuration.

RESULTS

The PAB3D code, along with the appropriate grids, has been applied to three separate configurations, the 2D nozzle of figure 1, the 3D nozzle ($3A_{12}B$) of figure 3, and the 3D nozzle with 24 tabs. There are two sets of test conditions (see Table I) provided by the NASA Glenn Research Center (GRC), one for the 2D case and one for the 3D cases. In addition, the $3A_{12}$ B configuration has been run for a second turbulence model and the 2D nozzle was run using both a set of experimental boundary conditions and the 3D test conditions. The six computer runs carried out are listed below:

Configuration/Tabs		Turbulence Model	Test Condition
2D	0	Std k-ε	1
2D	0	Std k-ε	Experimental
2D	0	Std k-ε	2
3D	12	Std k-ε	2
3D	12	SZL*	2
3D	24	Std k-ε	2

*Shih, Zhu, and Lumley eddy-viscosity model

The "experimental" flow conditions referred to above are P_t/P_{amb} = 1.7 for the fan flow, and P_t/P_{amb} = 1.48 for core flow. The ambient free-stream Mach number is 0.05.

Sample results are presented below for five configurations and two turbulence models with only the 2D nozzle with 3D boundary conditions excluded.

Axisymmetric nozzle

Figure 17 givens contour plots of the Mach numbers in and downstream of the 2D axisymmetric nozzle with the flow conditions of "Test Condition 1." Figure 17a gives these contours as lines of equal Mach number, while figure 17b gives the near-field contours as regions of the same Mach level, defined by the color key. The longitudinal dissipation and lateral spreading, characteristic of nozzle flows, can be clearly seen.

Figure 18 gives similar results for the 2D nozzle with the "Experimental" values for the core and fan pressure ratios. In this case, the fan flow Mach number is higher than that of the core and downstream flow velocities and lateral mixings (due to the fan flow) are both higher (see figures 17a and 18a) than that of figure 17. Note that the Mach-level key is different in figure 18 from that of figure 17.

$3A_{12}B$ Nozzle

Calculated results for the 3D twelve-tab configuration and the k-_ turbulence model at test condition is plotted in figure 19. Figure 19 includes seven color-contour plots of the following quantities:

- Symmetry plane Mach number — Figure 19a
- Cross plane Mach numbers at x = 100 mm and x = 500 mm — Figure 19b
- Symmetry plane turbulent kinetic energy — Figure 19c
- Cross plane turbulent kinetic energy at x = 100 mm and and x = 500 mm — Figure 19d
- Symmetry plane pressure ratio — Figure 19e
- Cross plane pressure ratio at x = 100 mm and x = 500 mm — Figure 19f
- Cross plane turbulent kinetic energy at x = 100 mm for three grid levels — Figure 19g

Several features are of interest with respect to these results:

- The small amount of shear between the core and fan flows (see figures 19a and 19c)
- The primary shear layer between the fan and free-stream flows (figure 19c)
- Cross plane plots of Mach number indicate a substantial effect due to the tabs (figures 19b)
- Crossplane plots of turbulent kinetic energy show large production around the fan/freestream interface (figure 19d).

- The near constant pressure downstream of the nozzle (figures 19e and 19f)
- Grid level reduction from 444 to 222 shows a significant difference in the turbulent kinetic energy. Further reduction to the 112 grid level has only a small effect (figure 19g)

Turbulence Model Effects

Figure 20 presents the same set of contour plots, as figure 19 except the turbulence model is that of Shih, Zhu and Lumley. Comparison of these results with those using the k-_ model yield the following observations:

- The symmetry plane Mach contours are essentially the same (figures 19a and 20a)
- Cross plane Mach contours are also similar (figures 19b and 20b)
- The k-_ model yields a higher level of turbulent energy between the fan and free-stream flows than the SZL model. Cross-plane plots of the turbulent energy show the same phenomena (figures 19d and 20d)
- The downstream pressures are very little different (figures 19e, 19f, 20e and 20f)
- Both the k-_ turbulence model and the SZL model show that there is a significant difference between the 444 and 222 grid levels for the turbulent kinetic energy while there is very little difference between 222 and 112 grid levels.

$3A_{24}B$ Nozzle

As noted earlier, a 24-tab grid and calculation was carried out using alternating in and out deflections similar to the 12-tab configuration. Since the 24 tabs had to fit the same circumference as the 12 tabs, the 24 tabs are half the size of the 12 tabs. Seven figures give these results as in the other 3D cases and are numbered 21a through 21g. The results are for the k-__turbulence model and consequently should be compared to figure 19. Test condition 2 was used as in the results for figures 19 and 20. It should be remembered that the 24-tab crossplane plots are given for a 15-degree sector and should be combined with the mirror image to compare to those of the 12-tab configuration.

Figure 21a shows that there is slightly more attenuation of the downstream symmetry-plane, fan-flow Mach number for the 24-tab configuration than the 12 tab. Cross plane Mach contours in figures 21b and 19b for x = 100 mm and x = 500 mm indicate similar patterns (although compressed) at x = 100 and slightly different patterns at x = 500 mm. Overall it appears that the 24-tab configuration produces slightly more Mach number reduction than the 12-tab. Figures 21c and 21d and figures 19c and 19d clearly show that the 12 tab configuration caused less turbulent energy between the free-stream and fan flows than the 24 tab (see figures 19d and 21d for x = 500 mm). Pressure ratio plots for the 24-tab configuration in figures 21e and 21f are roughly the same as those of 19e and 19f for the 12-tab geometry. Finally, the grid level sensitivity of the turbulent kinetic energy, shown in figure 21g, is about the same as in figure 19g. Calculated results and electronic files have been formulated for the axysymmetric nozzle with the 3D boundary conditions to enable a precise estimate of the effects of the tabs but no plots were made. Files for all six cases are detailed in Appendix C.

Concluding Remarks

Plug-nozzle/engine-exhaust, Navier-Stokes calculations have been carried out for three separate configurations, one 2D and two 3D. The latter are three dimensional due to the presence of mixer elements on the trailing edge of the core nozzle. A total of six N-S calculations were carried out to determine the effects of the turbulence model used, the grid size, 12 versus 24 mixer elements and the effects of the mixer elements themselves. Contour plots have been included for Mach number, turbulent kinetic energy and pressure ratio for a number of cases. Electronic files are available for all six cases.

List of Figures

Figure No.

1. Geometry of Baseline Axisymmetric Plug-Nozzle Configuration

2. G.E. Plug Nozzle with Alternating Inward and Outward Tabs (Configuration $3A_{12}B$) Core Nozzle.

3. Photograph of G.E. Plug Nozzle Showing Alternating Tabs on Core Nozzle.

4. Plug Nozzle Input Convention for Curves

5. Input Parameters for 2D Plug Nozzle Model

6. Automatically Generated Blocking for 2D Plug Nozzles

7. Blocking Numbers of the 2D Model (8 Blocks)

8. 2D Grid Detail

9. Updated 2D Model: Detail With New Parameters

10. Updated 2D Grid: Detail

11. Input Convention for Tab Edge Curves and Angle for 3D Model

12. Input Parameters for 3D Plug Nozzle Model with Tabs

13a. Automatically Generated 3D Surface Model for Nozzle with Tabs

13b. Surface Grid for Plug Nozzle with 12 Tabs (30 Degree Section)

14. Output Blocks for the 3D Model (9 Blocks)

15. Detail of 3D Model Grid on Symmetry Plane j-min

16. Grid of 3D Model on j-min Symmetry Plane

17a. PAB3D Solution for 2-D Nozzle. 212 Grid Level. Minf = 0.05, no fan flow, core flow pt/pamb = 1.19 - Lines of equal Mach number.

17b. PAB3D Solution for 2-D Nozzle. 212 Grid Level. Minf = 0.05, no fan flow, core flow pt/pamb = 1.19 - Equal Mach Zones.

18a. PAB3D Solution for 2-D Nozzle. 212 Grid Level. Minf = 0.05, fan flow pt/pamb = 1.7, core flow pt/pamb = 1.48 - Lines of equal Mach number.

18b. PAB3D Solution for 2-D Nozzle. 212 Grid Level. Minf = 0.05, fan flow pt/pamb = 1.7, core flow pt/pamb = 1.48 - Equal Mach zones.

19a. Twelve Tab, PAB3D 3-D Nozzle Solution, 112 Grid Level. Std. $\kappa-\varepsilon$ turbulence model, symmetry plane (j = jmax). – Equal Mach zones in symmetry plane.

19b. Twelve Tab, PAB3D Solution for 3-D Nozzle, 112 Grid Level. Std. $\kappa-\varepsilon$ turbulence model, constant i planes – Equal Mach at x = 100 and 500 mm.

19c. Twelve Tab, PAB3D 3-D Nozzle Solution, 112 Grid Level. Std. $\kappa-\varepsilon$ turbulence model, symmetry plane (j = jmax). – Equal turbulent energy zones in symmetry plane.

19d. Twelve Tab, PAB3D Solution for 3-D nozzle, 112 Grid Level. Std. $\kappa-\varepsilon$ turbulence model, constant i planes – Equal turbulent energy zones at x = 100 and 500 mm.

.

19e. Twelve Tab, PAB3D 3-D Nozzle Solution, 112 Grid Level. Std. $\kappa-\varepsilon$ turbulence model, symmetry plane (j = jmax). – Equal pressure zones in symmetry plane.

19f. Twelve Tab, PAB3D Solution for 3-D Nozzle, 112 Grid Level. Std. $\kappa-\varepsilon$ turbulence model, constant i planes – Equal pressure zones at x = 100 and 500 mm.

19g. Twelve Tab, PAB3D Solution for 3-D Nozzle, 112 Grid Level. Std. $\kappa-\varepsilon$ turbulence model, constant i planes – Effect of grid size on turbulent energy

at x = 100.

20a. Twelve Tab, PAB3D 3-D Nozzle Solution, 112 Grid Level. SZL turbulence model, symmetry plane (j = jmax) - Equal Mach zones in symmetry plane.

20b. Twelve Tab, PAB3D Solution for 3-D Nozzle, 112 Grid Level. SZL turbulence model, constant i planes - Equal Mach zones at x = 100 and 500 mm.

20c. Twelve Tab, PAB3D 3-D Nozzle Solution, 112 Grid Level. SZL turbulence model, symmetry plane (j = jmax) - Equal turbulent energy zones in symmetry plane.

20d. Twelve Tab, PAB3D Solution for 3-D nozzle, 112 Grid Level. SZL turbulence model, constant i planes - Equal turbulent energy zones at x = 100 and 500 mm.

20e. Twelve Tab, PAB3D 3-D Nozzle Solution, 112 Grid Level. SZL turbulence model, symmetry plane (j = jmax) - Equal pressure zones in symmetry plane.

20f. Twelve Tab, PAB3D Solution for 3-D nozzle, 112 Grid Level. SZL turbulence model, constant i planes - Equal pressure zones at x = 100 and 500 mm.

20g. Twelve Tab, PAB3D Solution for 3-D nozzle, SZL turbulence model, constant i planes – Effect of grid size on turbulent energy at x = 100.

21a. Twenty Four Tab, 3D Configuration, 112 Grid Level. Std. $\kappa-\varepsilon$ turbulence model, symmetry plane (j = jmax) – Equal Mach zones in symmetry plane.

21b. Twenty Four Tab, 3D Configuration, 112 Grid Level. Std. $\kappa-\varepsilon$ turbulence model, constant i planes – Equal Mach zones at x = 100 and 500 mm.

21c. Twenty Four Tab, 3D Configuration, 112 Grid Level. Std. $\kappa-\varepsilon$ turbulence model, symmetry plane (j = jmax) – Equal turbulent energy zones in symmetry plane.

21d. Twenty Four Tab, 3D Configuration, 112 Grid Level. Std. $\kappa-\varepsilon$ turbulence model, constant i planes – Equal turbulent energy zones at x = 100 and 500 mm.

21e. Twenty Four Tab, 3D Configuration, 112 Grid Level. Std. $\kappa-\varepsilon$ turbulence model, symmetry plane (j = jmax) – Equal pressure zones in symmetry plane.

21f. Twenty Four Tab, 3D Configuration, 112 Grid Level. Std. $\kappa-\varepsilon$ turbulence model, constant i planes – Equal pressure zones at x = 100 and 500 mm.

21g. Twenty Four Tab, 3D Configuration. Std. $\kappa-\varepsilon$ turbulence model, constant i planes – Effect of grid size on turbulent energy at x = 100.

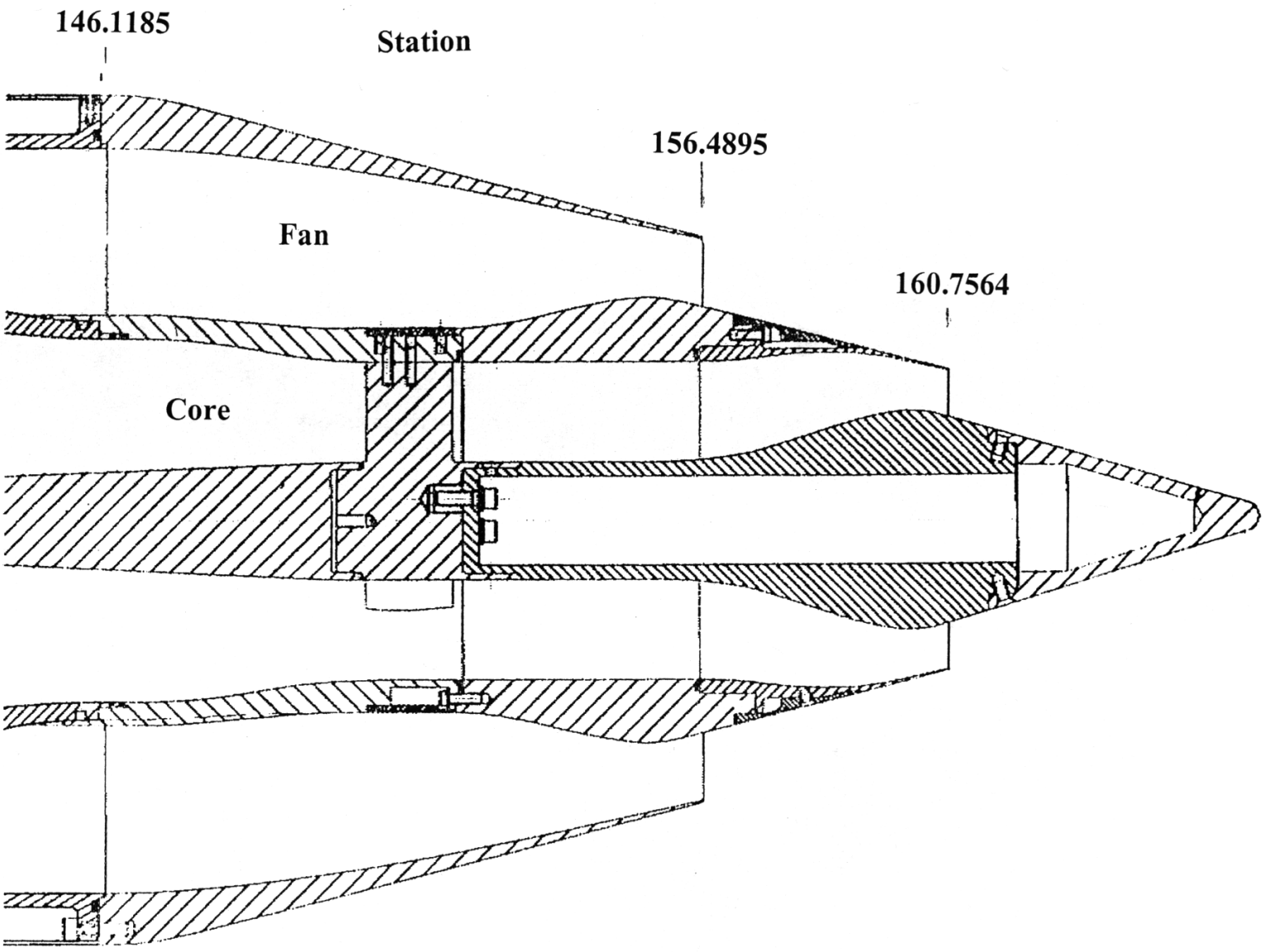

Figure 1. – Geometry of baseline axisymmetric plug-nozzle configuration.

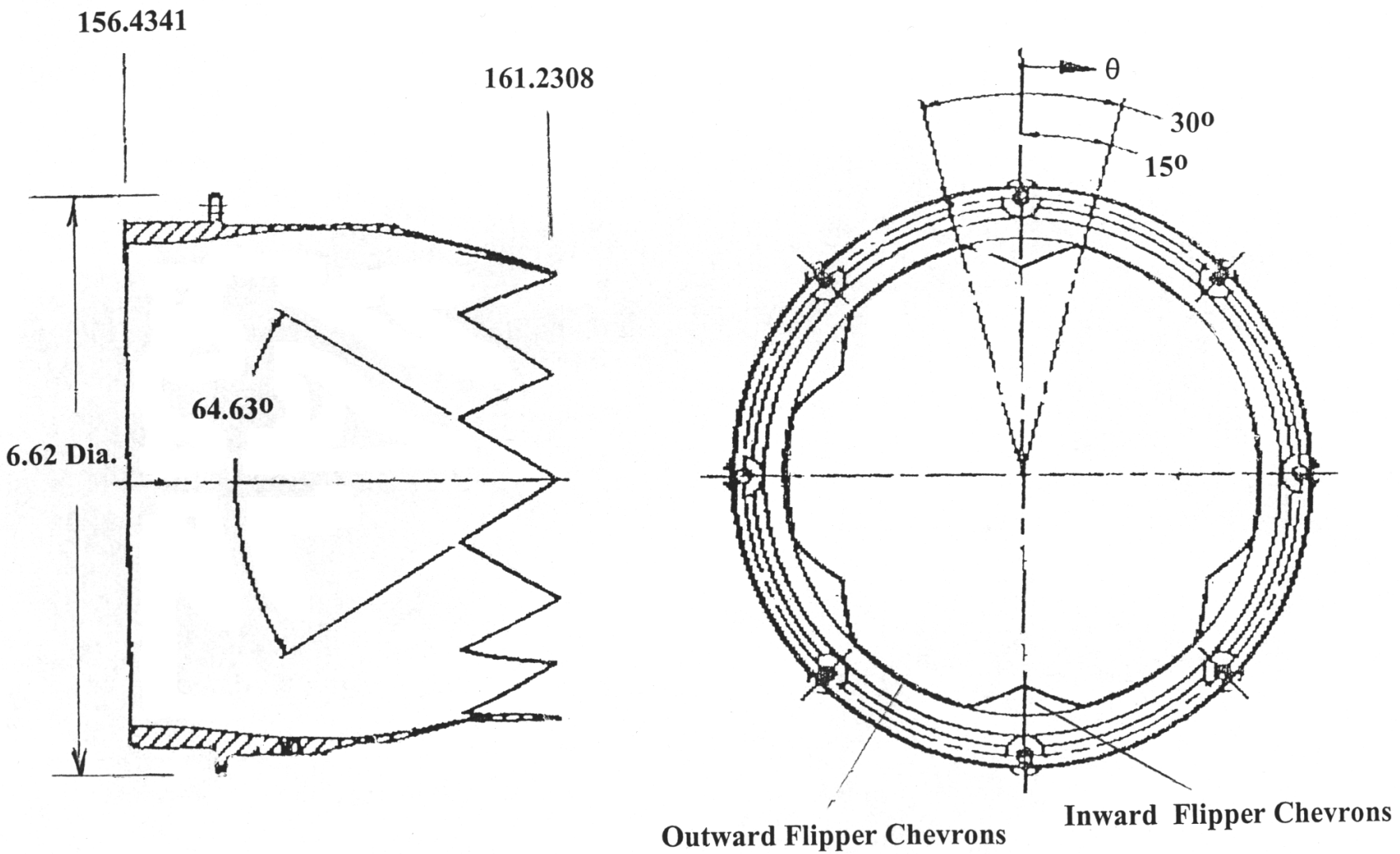

Figure 2. - G.E. Plug nozzle with alternating inward and outward tabs (Configuration $3A_{12}B$) core nozzle.

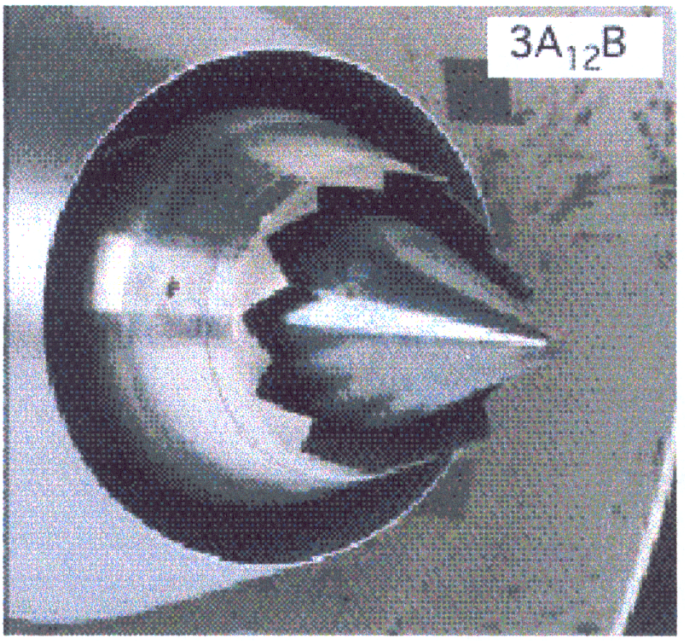

Figure 3. - Photograph of G.E. plug nozzle showing alternating tabs on core nozzle.

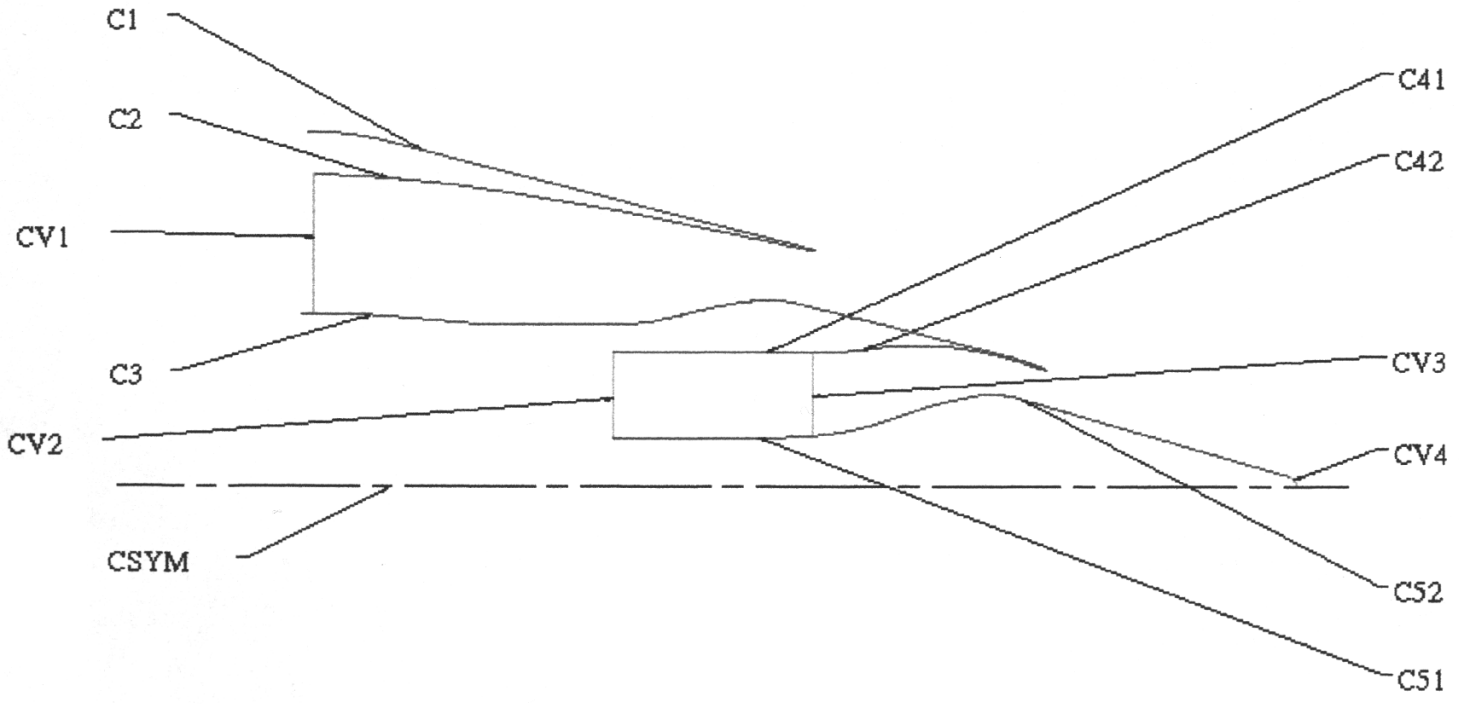

Figure 4. - Plug Nozzle Input Convention for Curves

Input parameter	Comment	Default Value
K-R1	factor times nacelle -length for distance on outer wall to collapse to thin wall	0.01
K_R2	factor times nacelle -length for distance on inner wall to collapse to thin wall	0.01
K_OP	Opening factor of grid at 4*DF in J direction	2.5
K_OP2	Opening factor of grid at plug in J direction	2.2

The length and the height of the doamin are internally defined by factors of the fan diameter DF. (see Figure
That can be changed to user defined factors very easily.

Figure 5. - Input Parameters for 2D Plug Nozzle Model

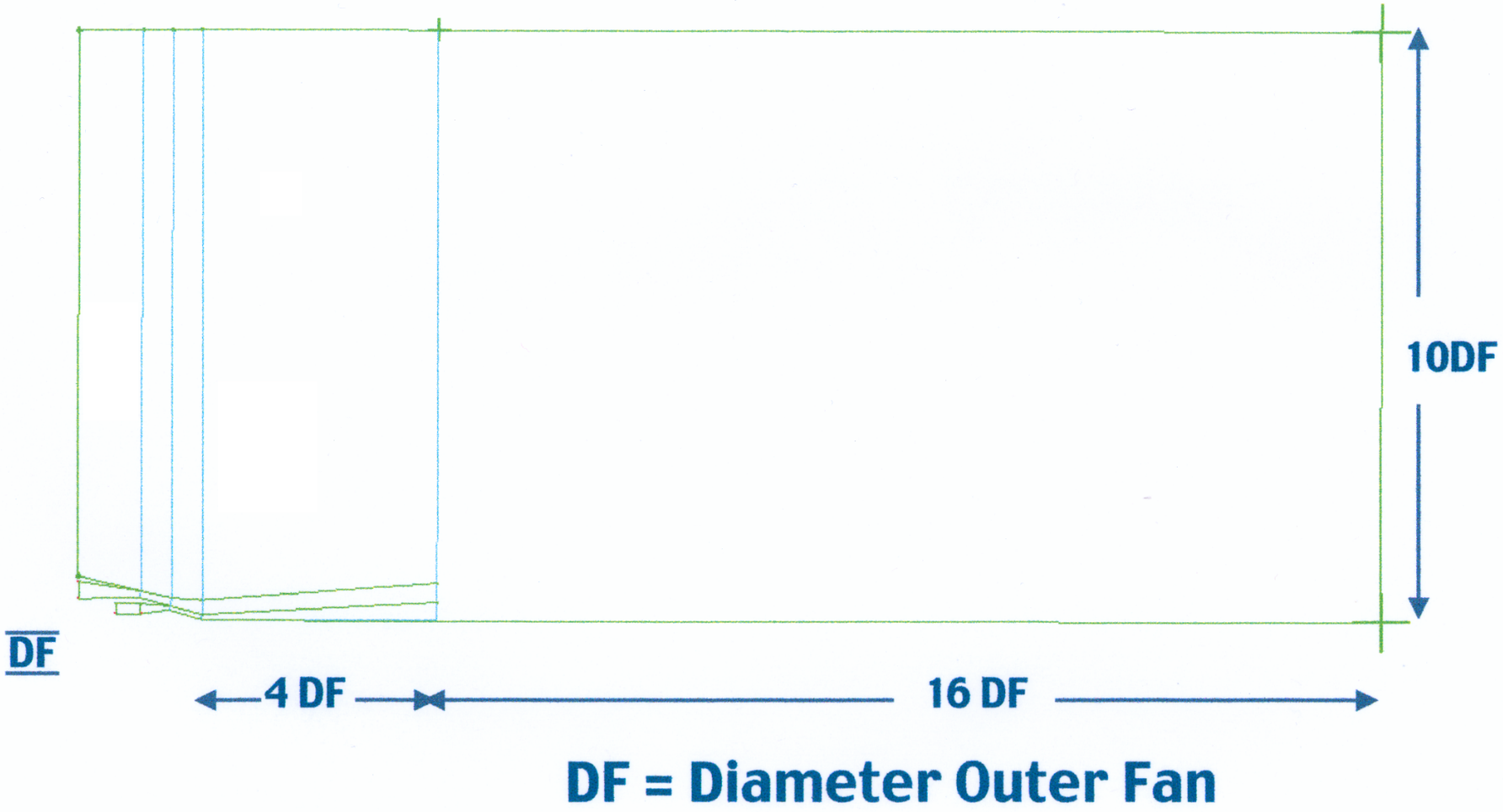

Figure 6. - Automatically Generated Blocking for 2D Plug Nozzle

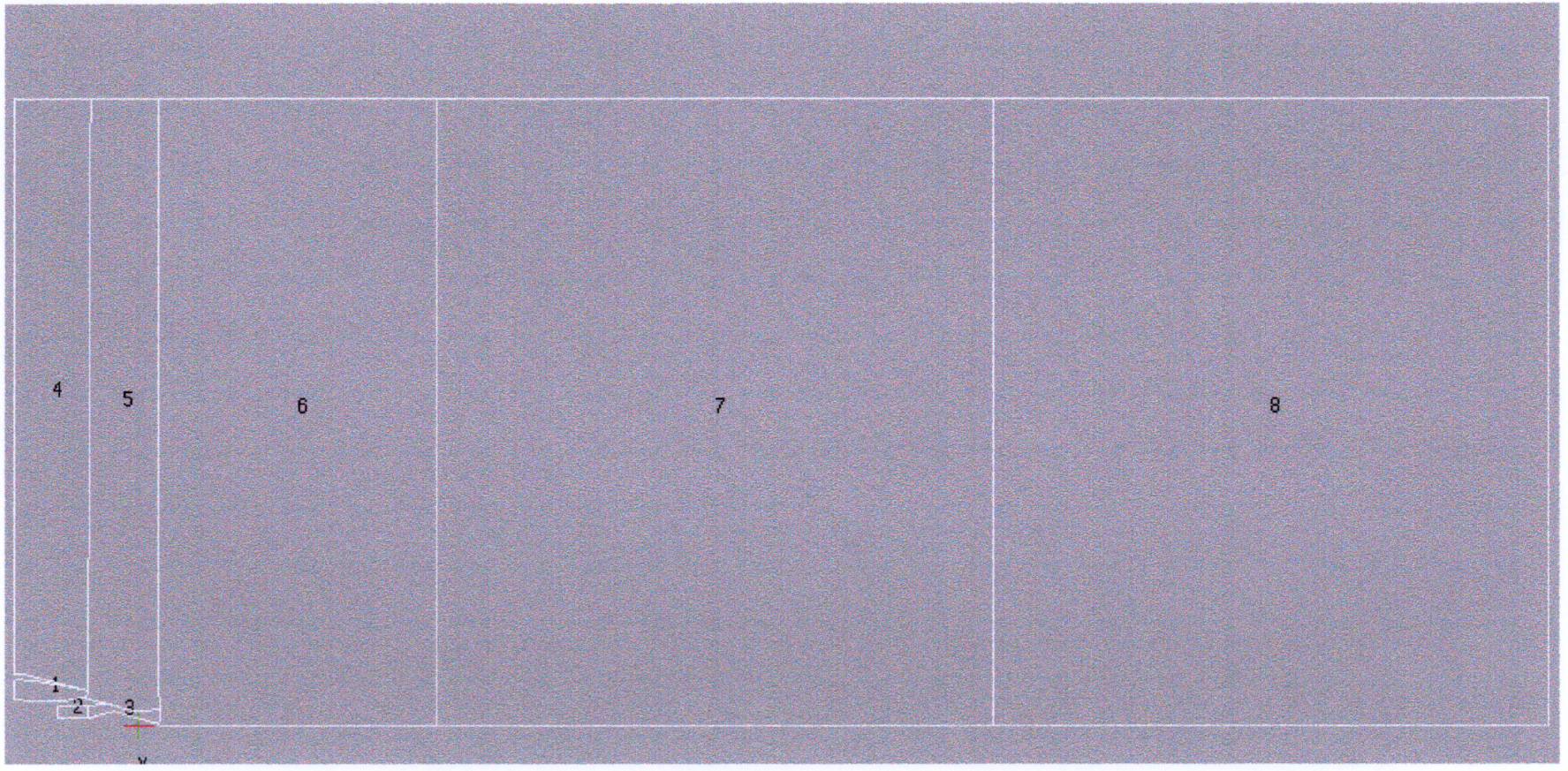

Figure 7. - Blocking Numbers of the 2D Model (8 Blocks)

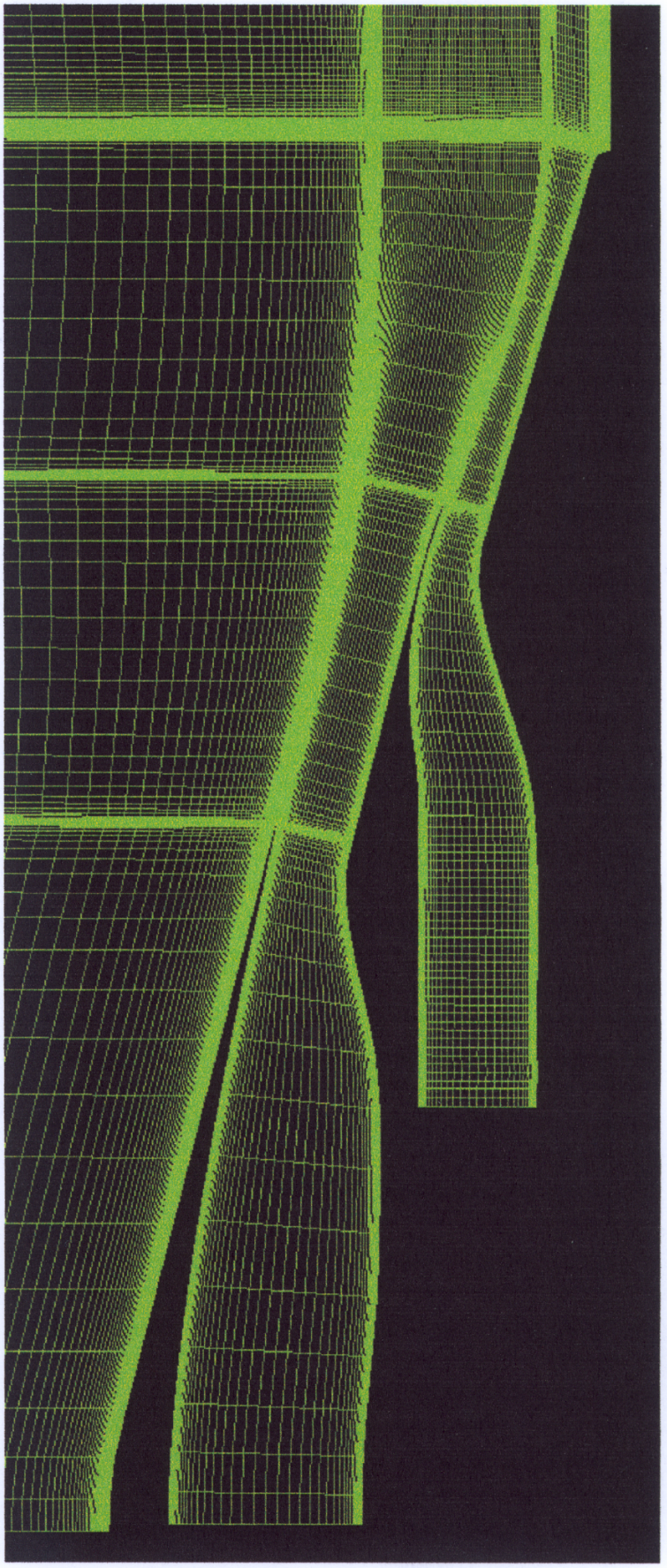

Figure 8. - 2D Grid Detail

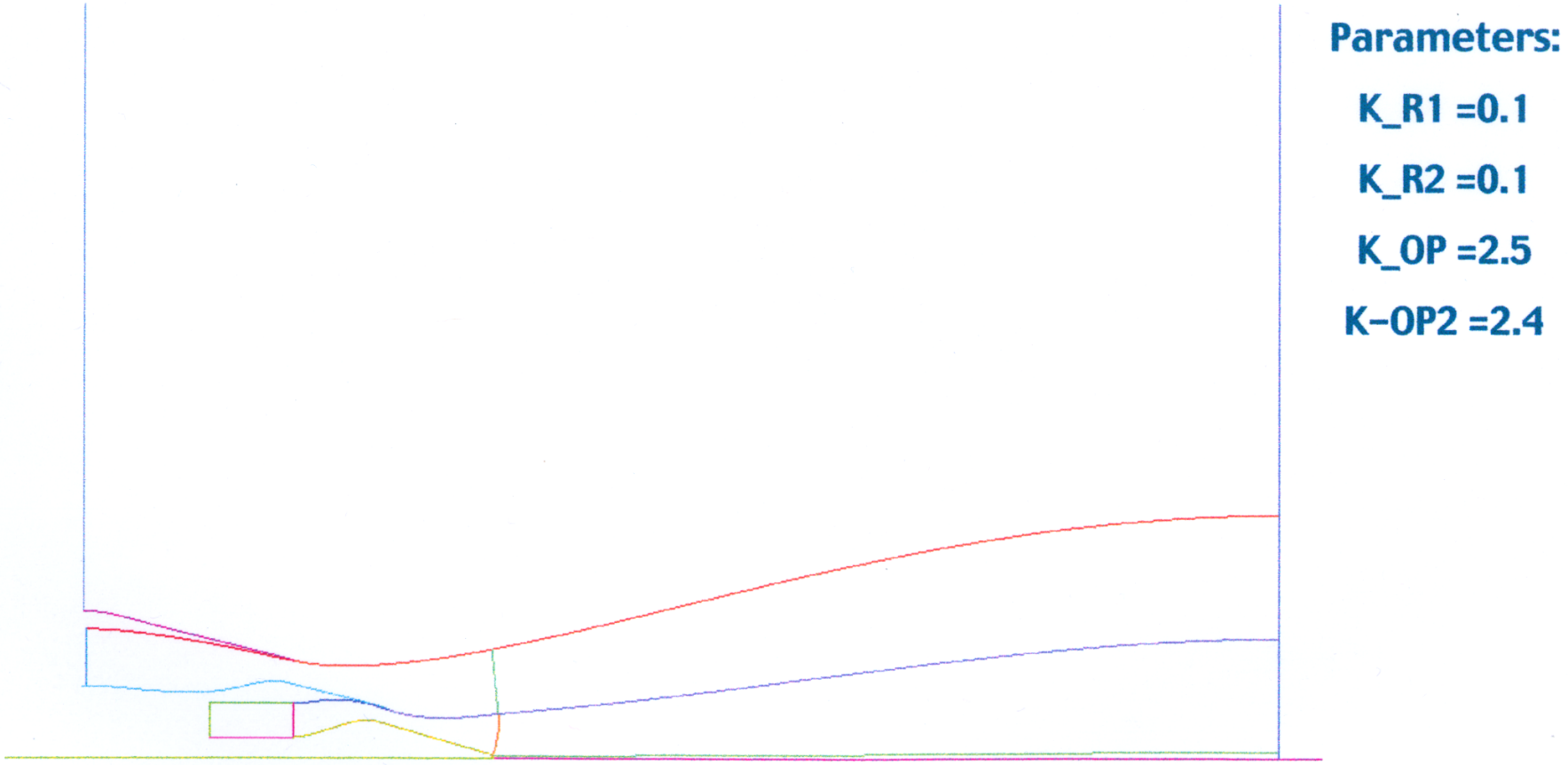

Figure 9. - Updated 2D Model: Detail with new Parameters

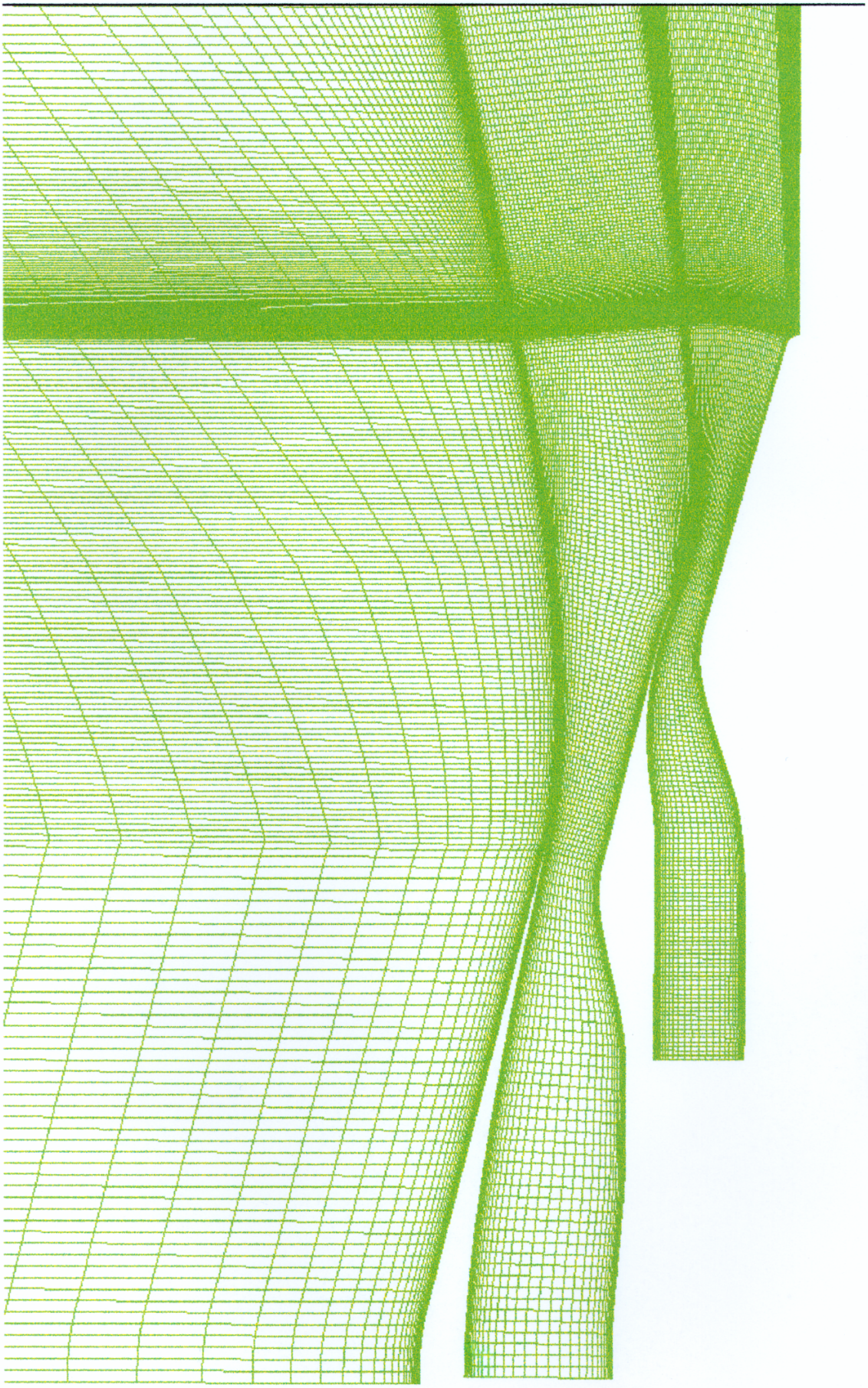

Figure 10. - Updated 2D Grid: Detail

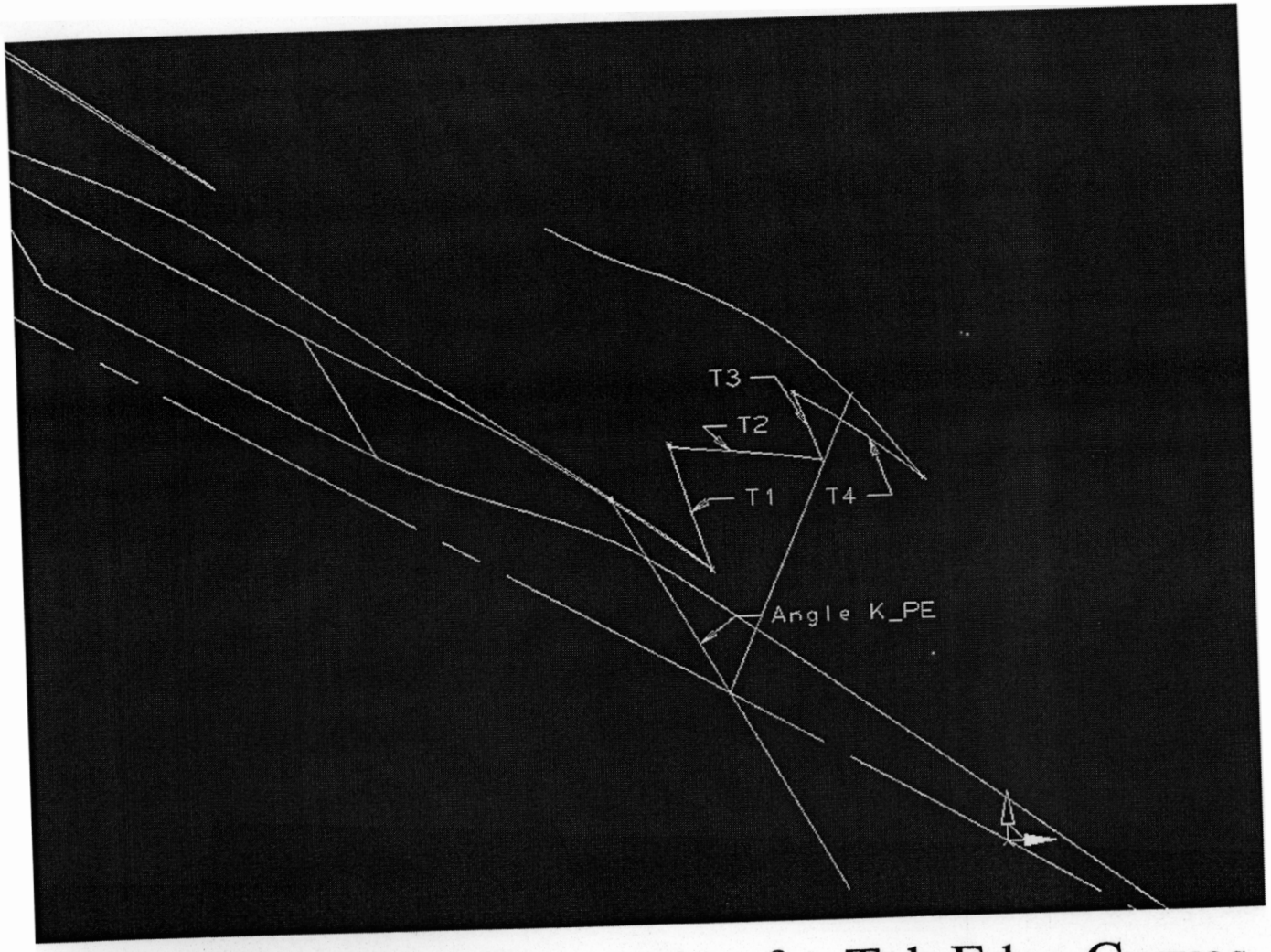

Figure 11. - Input Convention for Tab Edge Curves and Angle for 3D Model

Input Parameters	Comment	Default Value
K-R1	factor times nacelle -length for distance on outer wall to collapse to thin wall	0.025
K-R1	factor times nacelle -length for distance on inner wall to collapse to thin wall. Needs only to be defined once.	0.025
K_R2	dummy value (since 3D case is developed from 2D case) please leave at:	0.01
K_OP	Opening factor of grid at 4*DF in J direction	2.5
K_OP2	Opening factor of grid at plug in J direction	2.2
K_PE	Openig angle for 2 tabs with center axis (see Figure 9)	60
The length and the height of the domain are internally defined by factors of the fan diameter DF. (see Figure 3)		
That can be changed to user defined factors very easily.		

Figure 12. - Input Parameters for 3D Plug Nozzle Model with Tabs

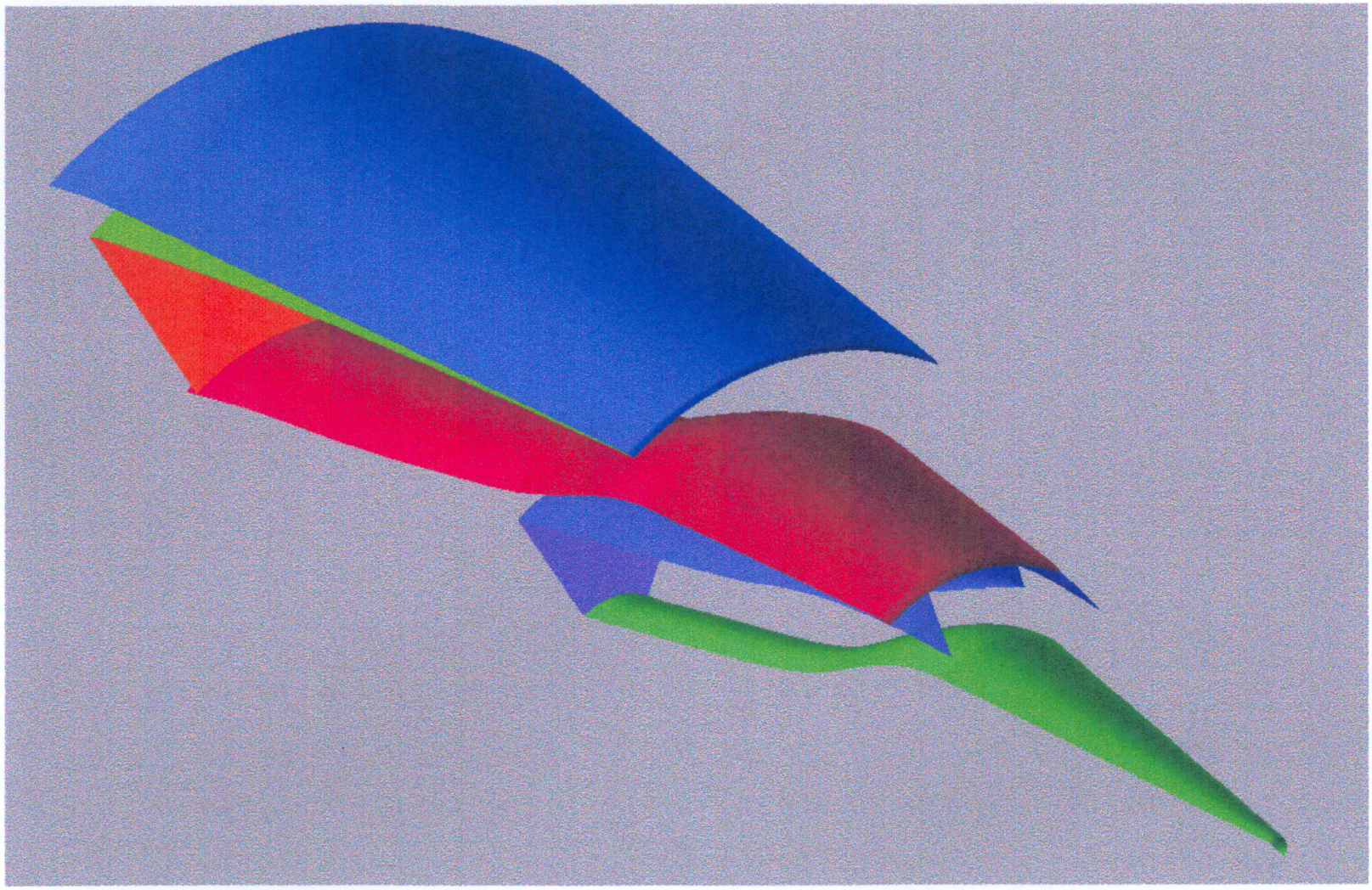

Figure 13a. - Automatically Generated 3D Surface Model for Nozzle with Tabs

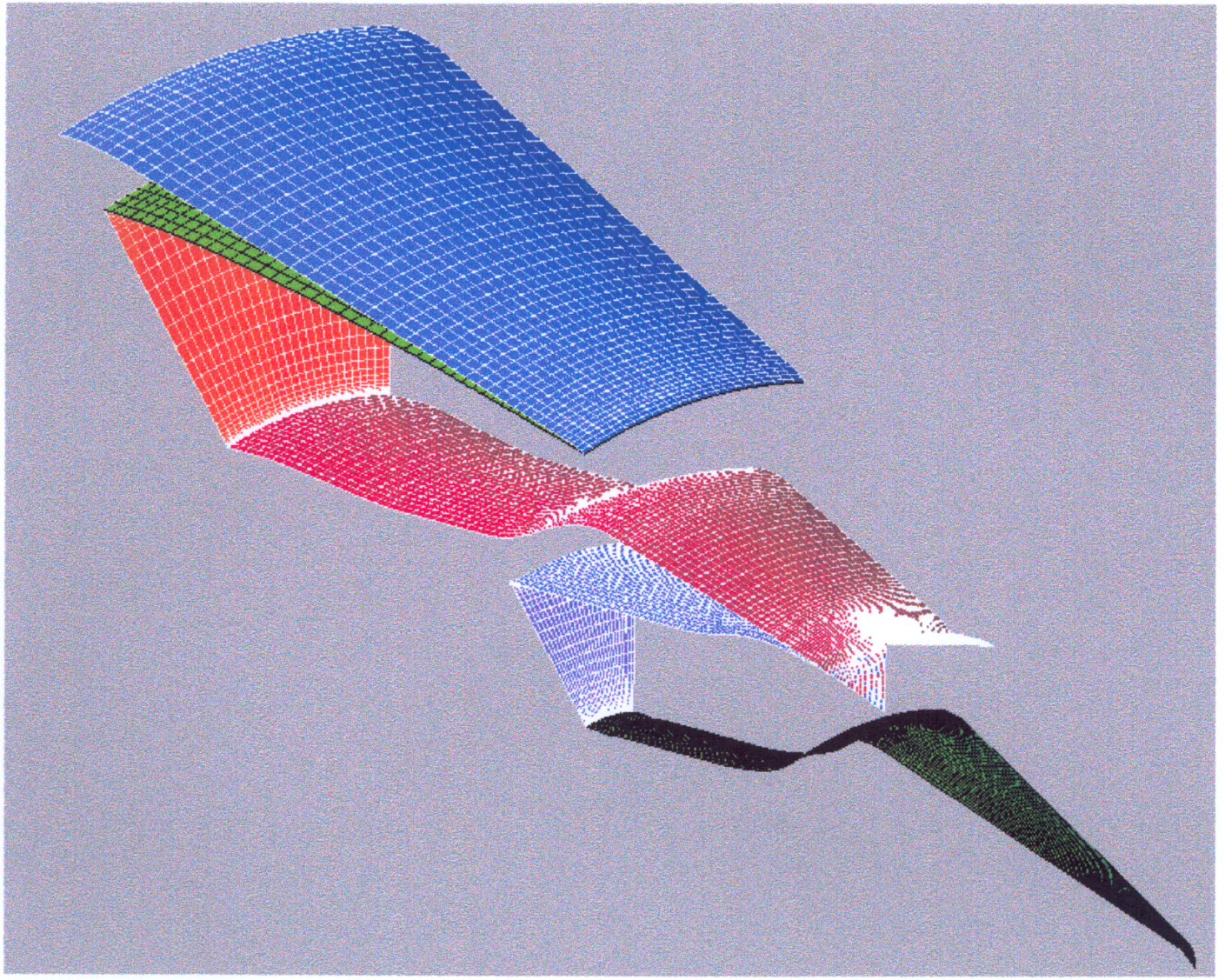

Figure 13b. - Surface Grid for Plug Nozzle with 12 Tabs (30 Degree Section)

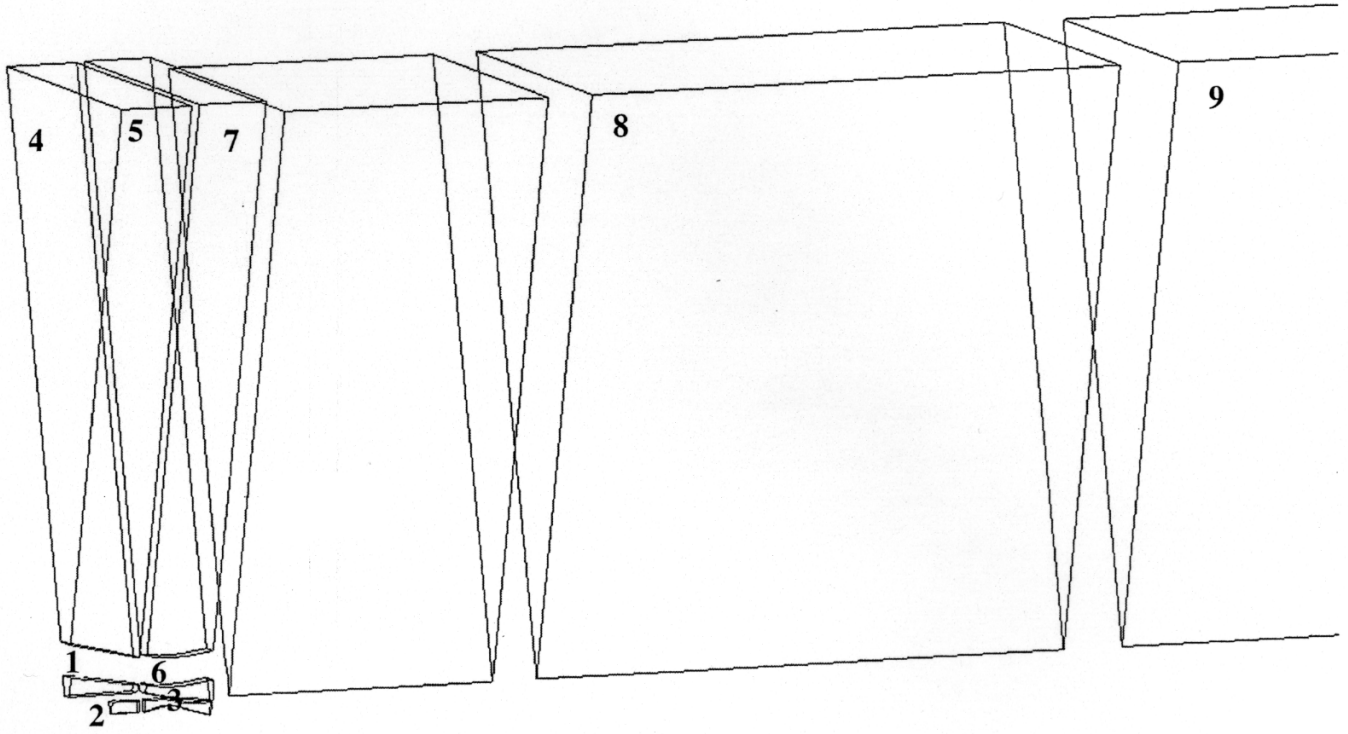

Figure 14. - Output Blocks for the 3D Model (9 Blocks)

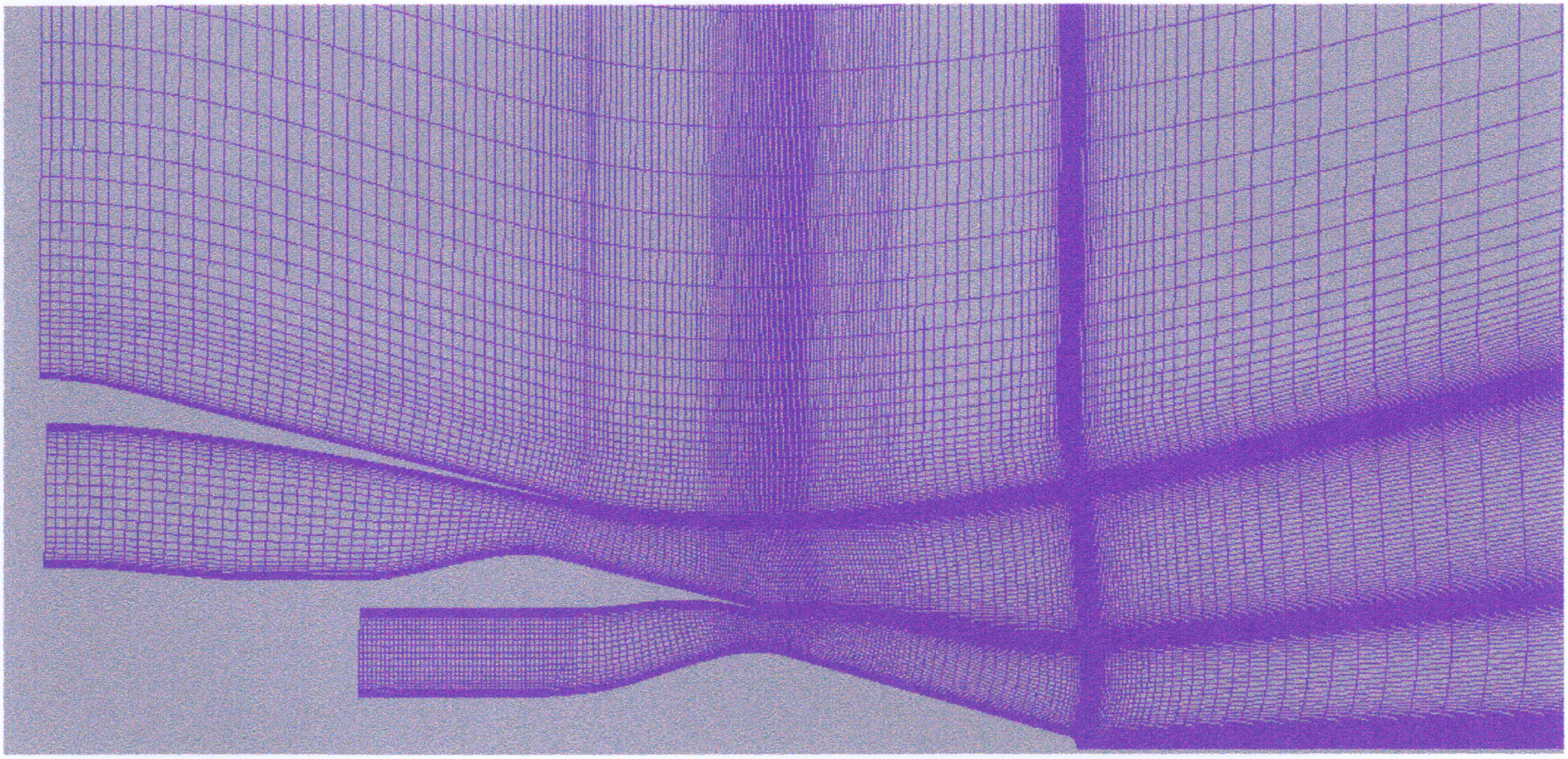

Figure 15. - Detail of 3D Model Grid on Symmetry Plane j-min

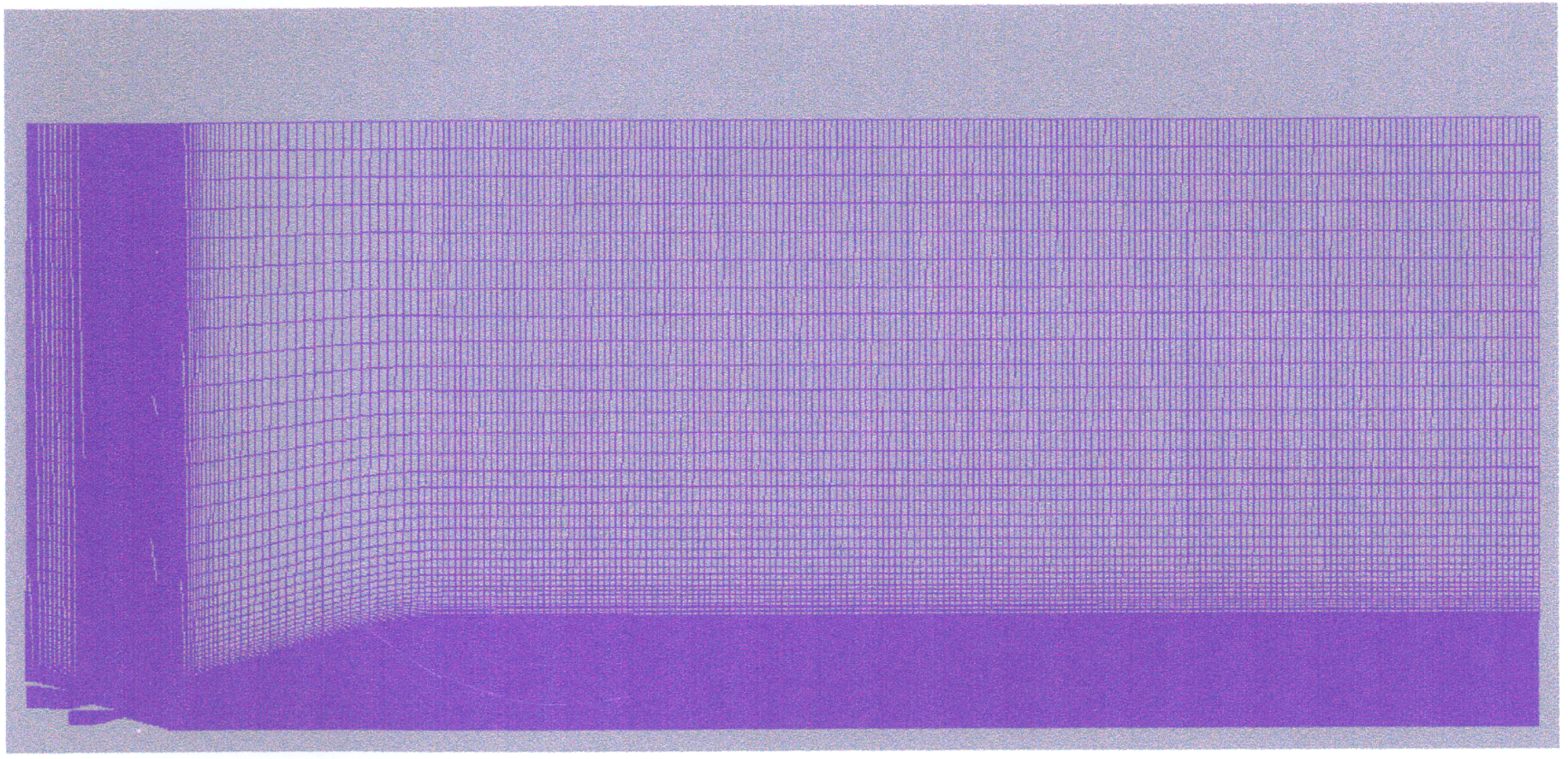

Figure 16. - Grid of 3D Model on j-min Symmetry Plane

Figure 17. – PAB3D solution for 2-D nozzle. 212 grid level.
Minf=0.05, no fan flow, core flow pt/pamb = 1.19

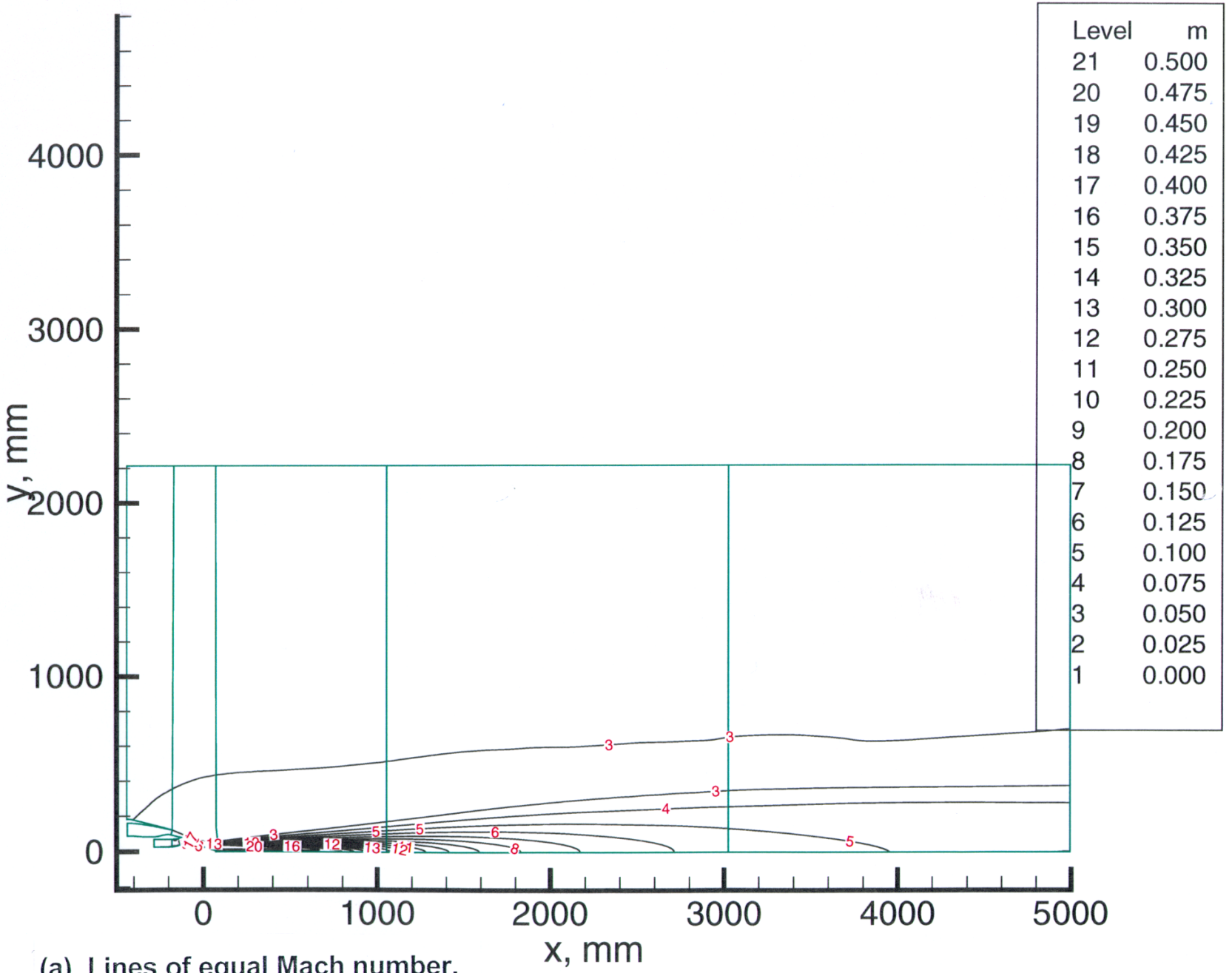

(a) Lines of equal Mach number.

Figure 17. – PAB3D solution for 2-D nozzle. 212 grid level.
Minf=0.05, no fan flow, core flow pt/pamb = 1.19

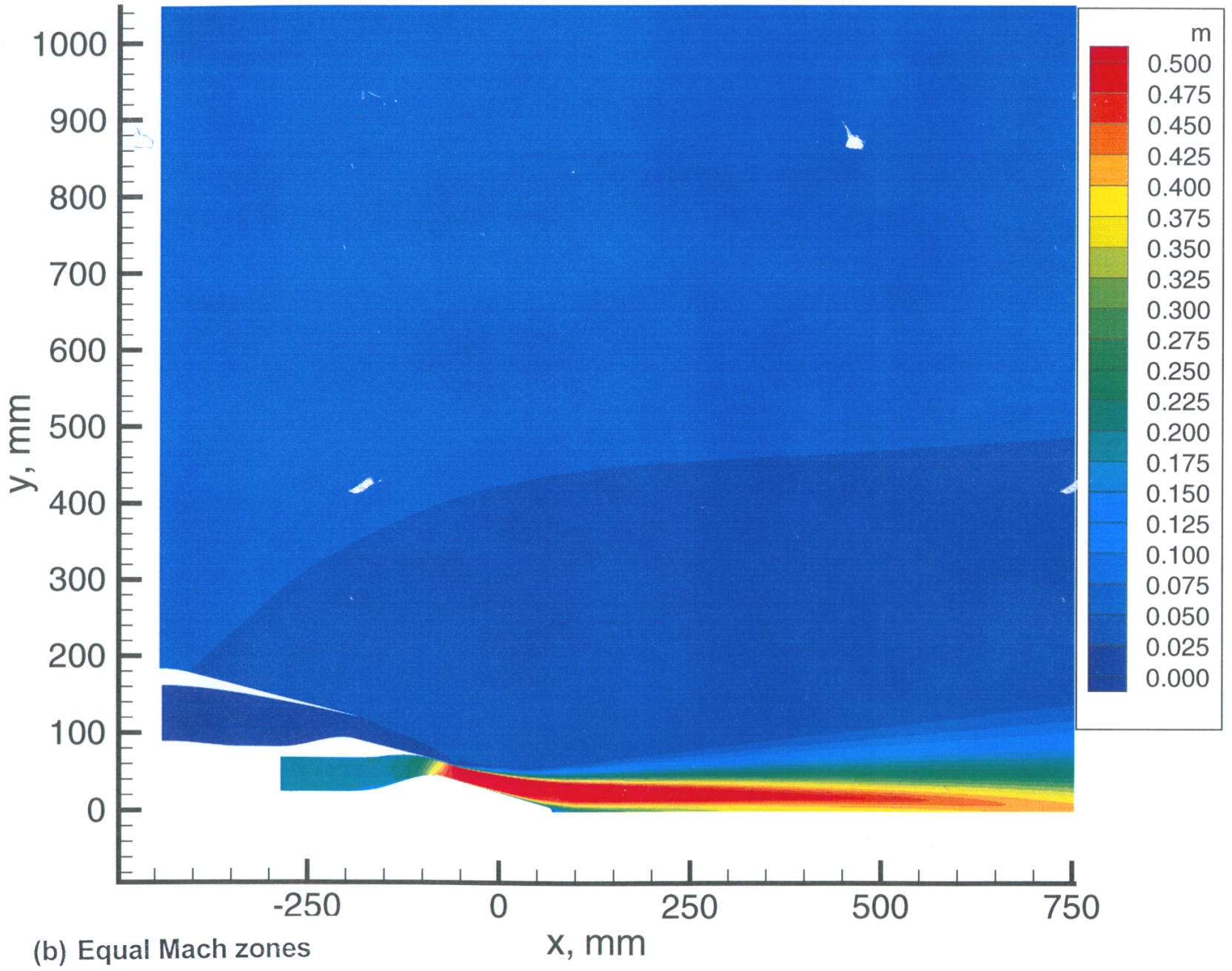

(b) Equal Mach zones

Figure 18. – **PAB3D solution for 2-D nozzle. 212 grid level. Minf=0.05, fan flow pt/pamb = 1.7, core flow pt/pamb = 1.48**

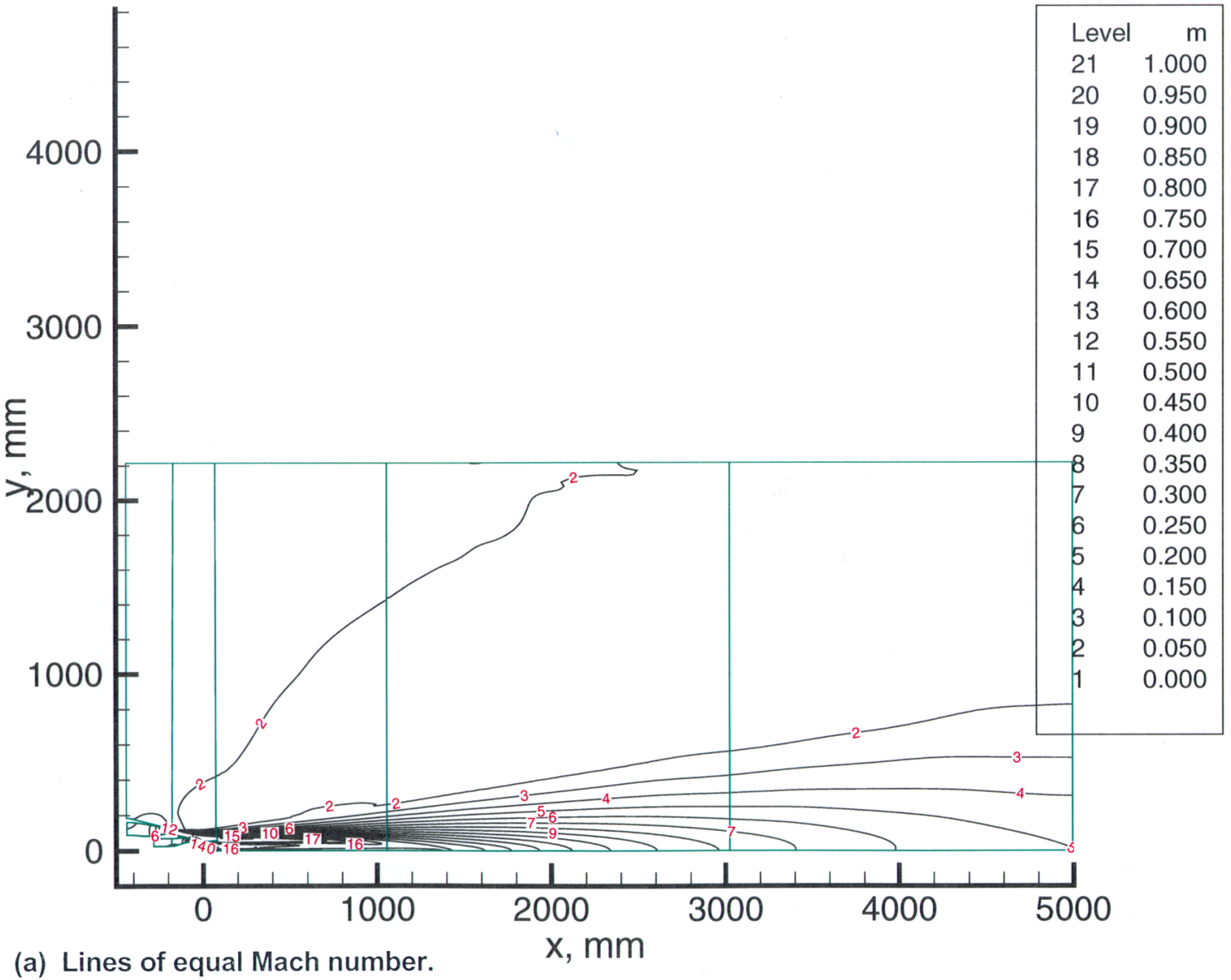

(a) Lines of equal Mach number.

Figure 18. – PAB3D solution for 2-D nozzle. 212 grid level.
Minf=0.05, fan flow pt/pamb = 1.7, core flow pt/pamb = 1.48

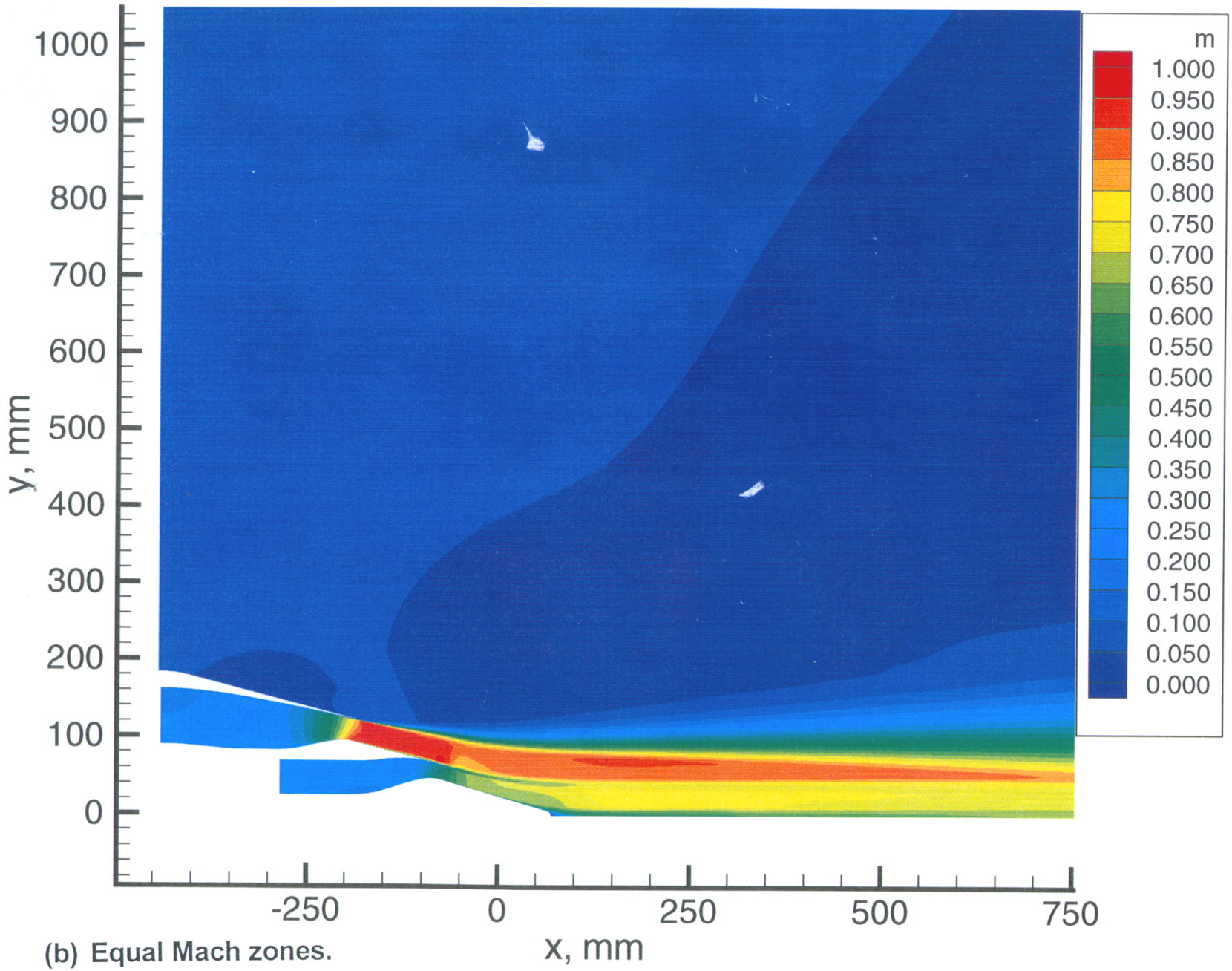

(b) Equal Mach zones.

Figure 19. - Twelve tab, PAB3D 3-D nozzle solution, 112 grid level.
Std. k-ε turbulence model, symmetry plane (j=jmax)

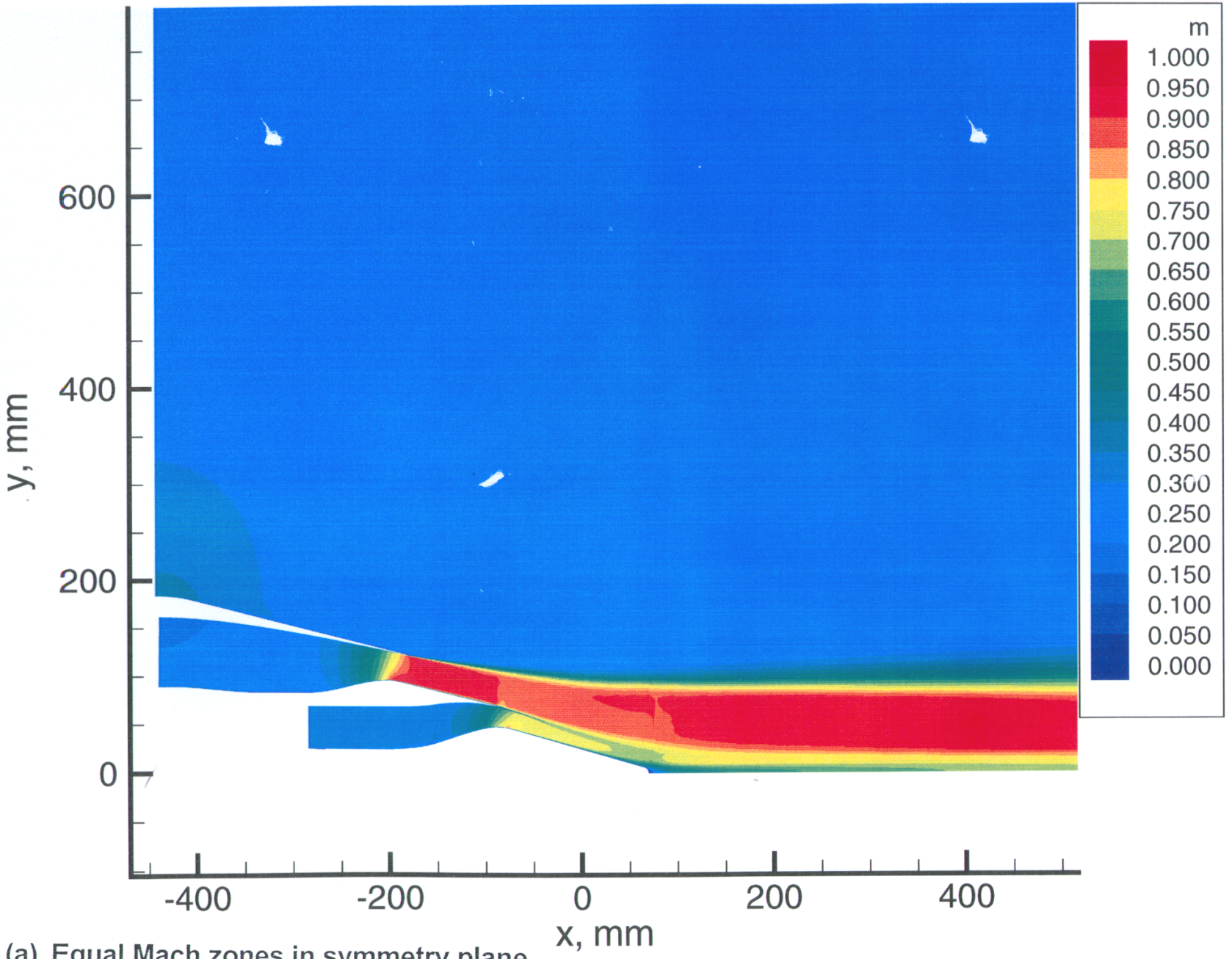

(a) Equal Mach zones in symmetry plane.

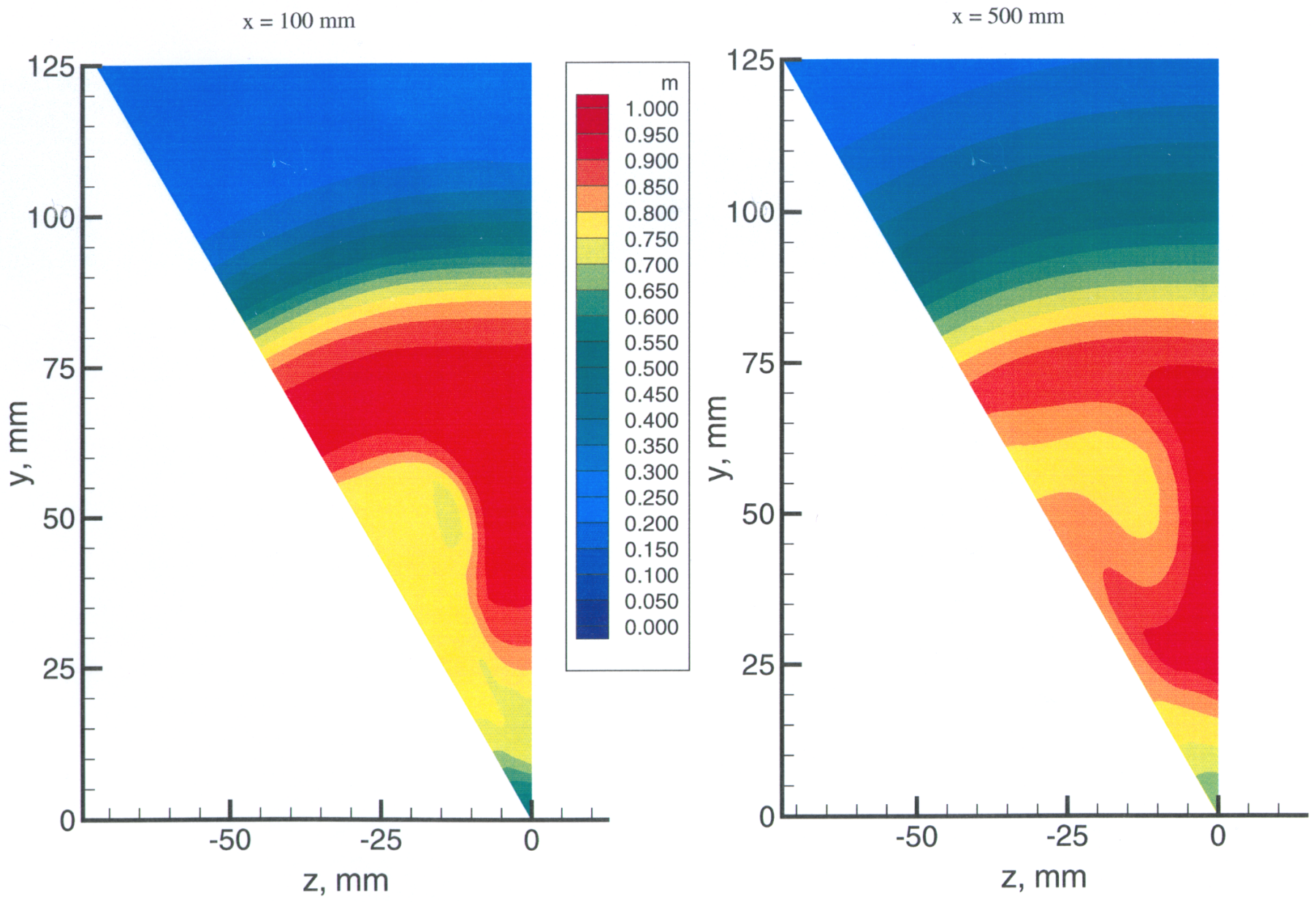

Figure 19. - Twelve tab, PAB3D solution for 3-D nozzle, 112 grid level. Std. k-ε turbulence model, constant i planes.

(b) Equal Mach zones at x = 100 and 500 mm.

Figure 19. - Twelve tab, PAB3D 3-D nozzle solution, 112 grid level.
Std. k-ε turbulence model, symmetry plane (j=jmax)

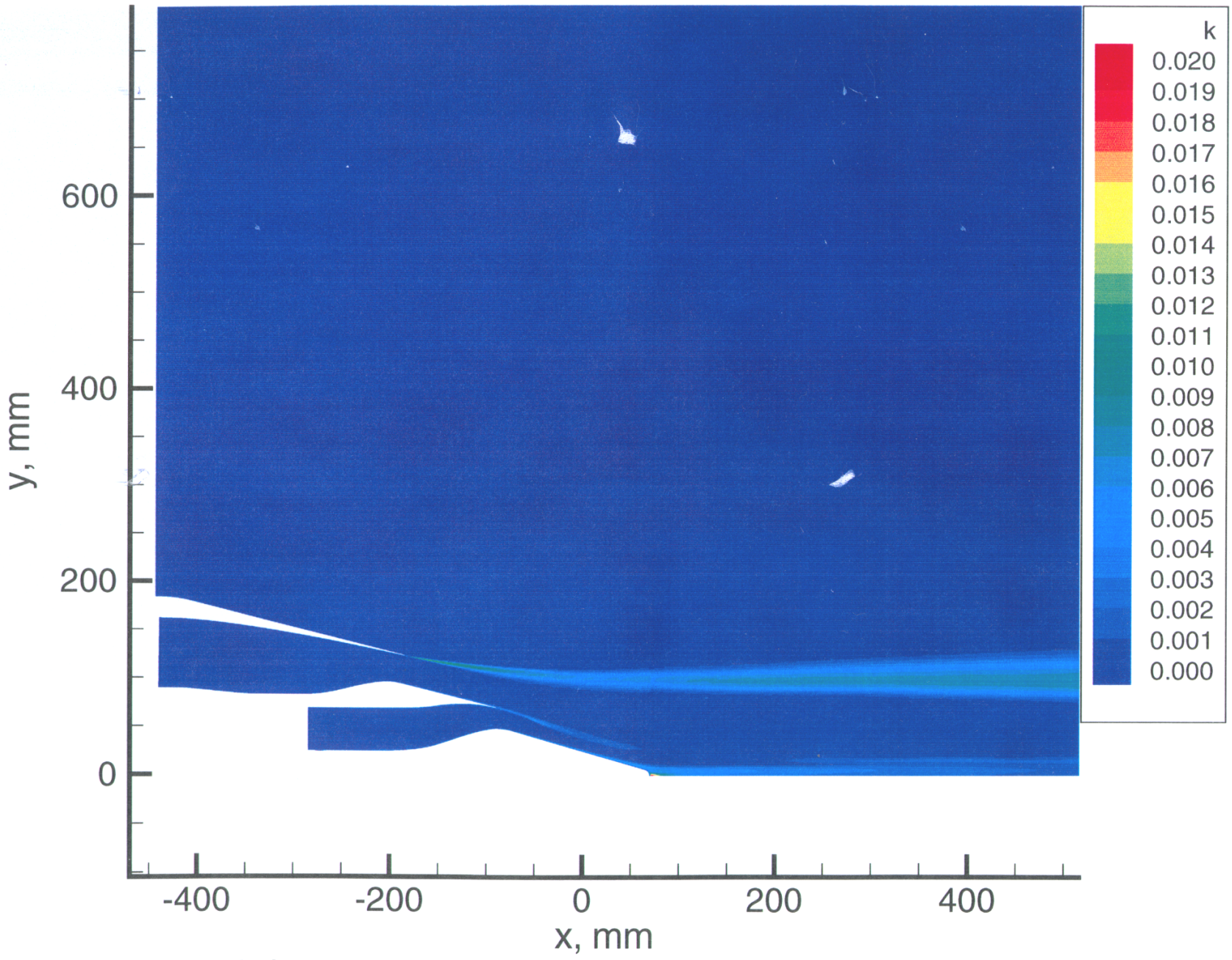

(c) Equal turbulent energy zones in symmetry plane.

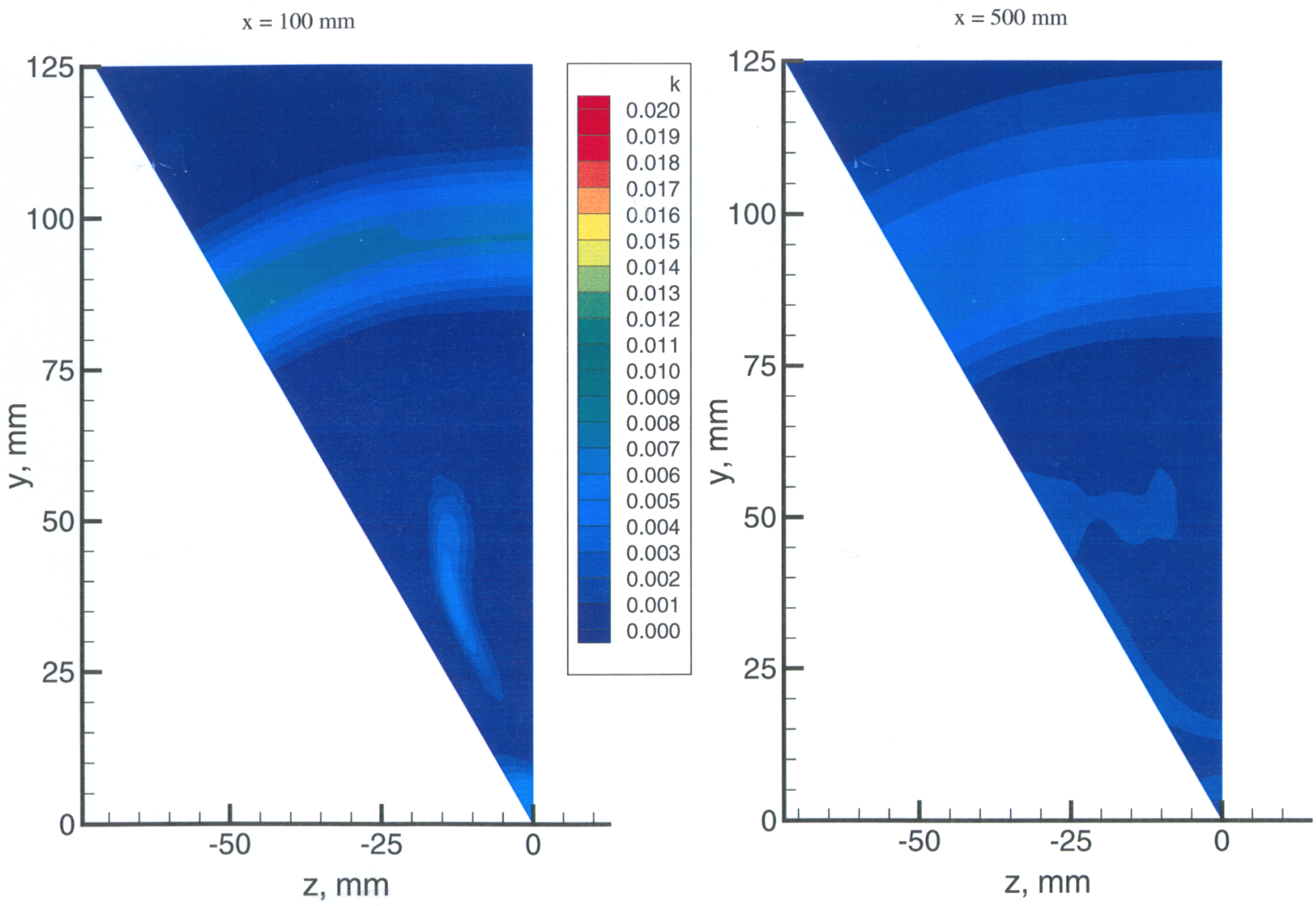

Figure 19. - Twelve tab, PAB3D solution for 3-D nozzle, 112 grid level. Std. k-ε turbulence model, constant i planes.

(d) Equal turbulent energy zones at x = 100 and 500 mm.

Figure 19. - Twelve tab,PAB3D 3-D nozzle solution, 112 grid level.
Std. k-ε turbulence model, symmetry plane (j=jmax)

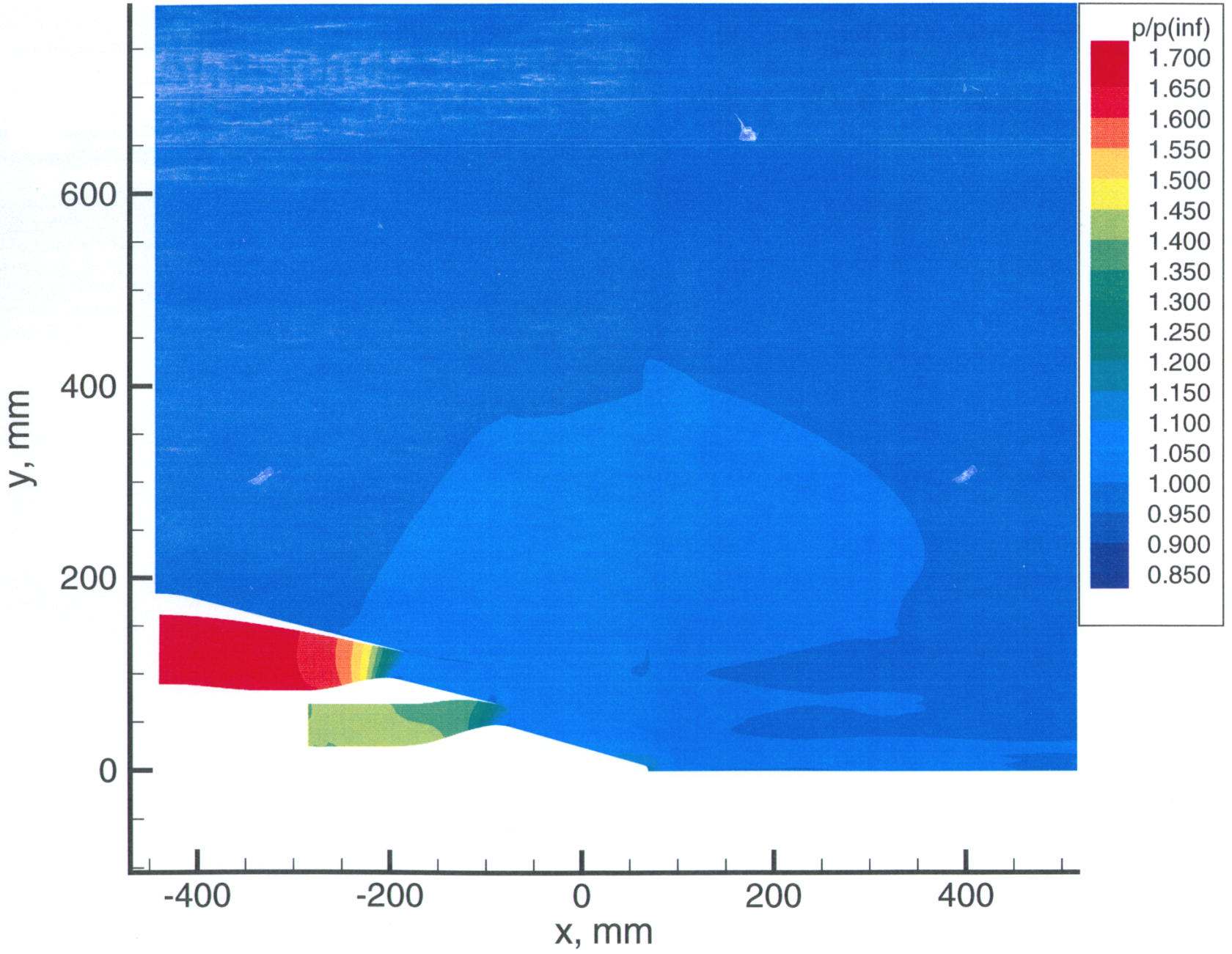

(e) Equal pressure zones in symmetry plane.

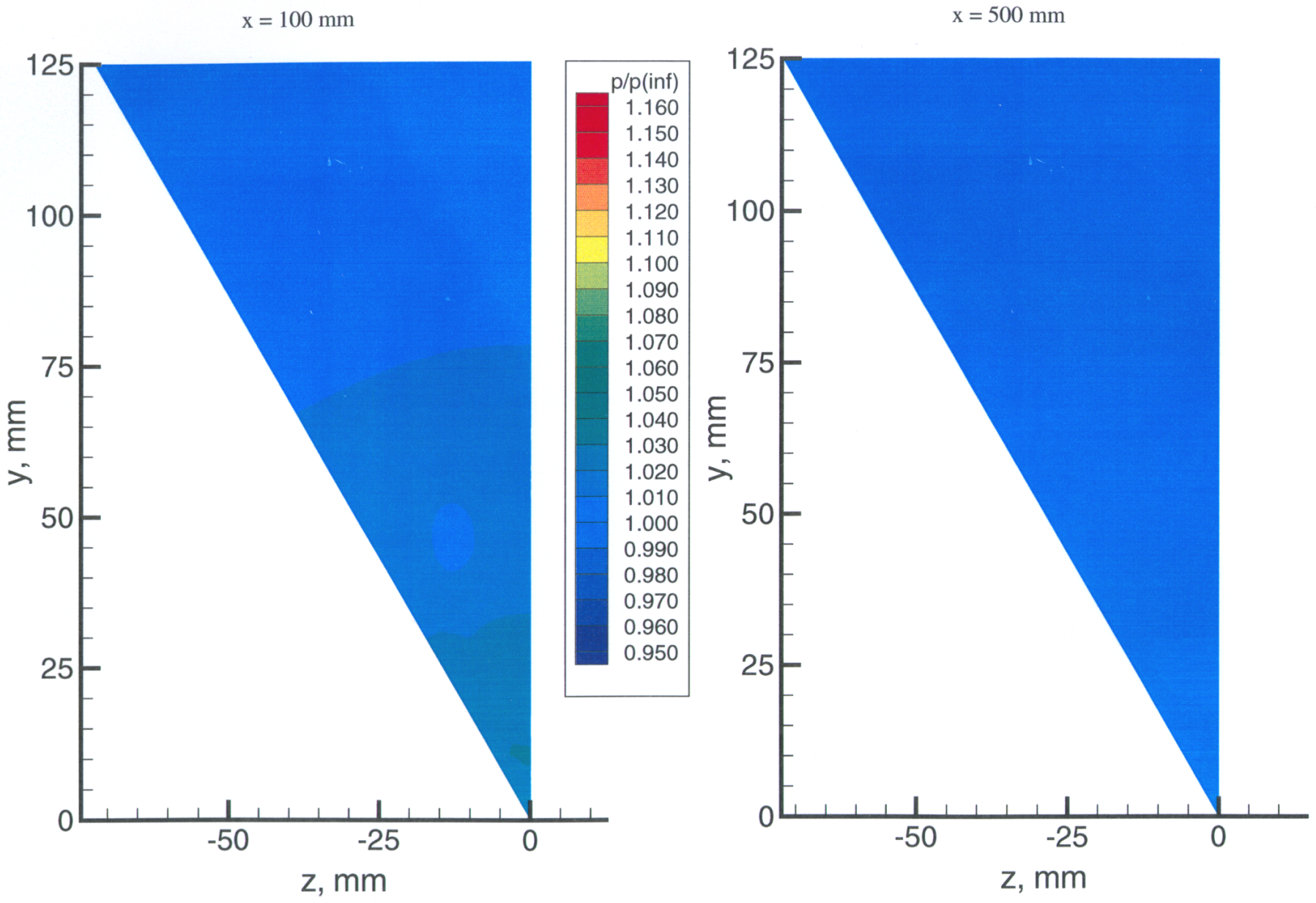

Figure 19. - Twelve tab, PAB3D solution for 3-D nozzle, 112 grid level. Std. k-ε turbulence model, constant i planes.

(f) Equal pressure zones at x = 100 and 500 mm.

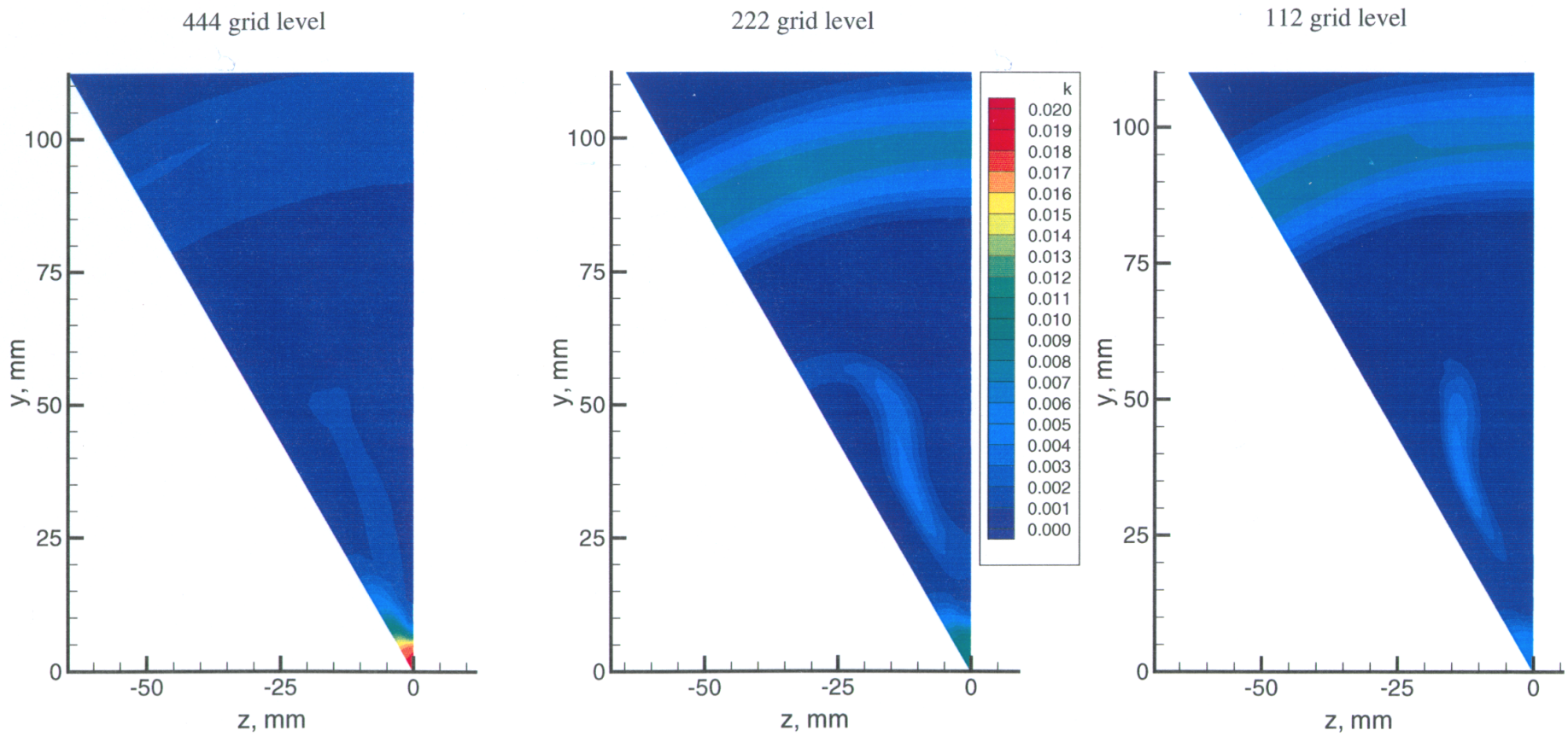

Figure 19. - Twelve tab, PAB3D solution for 3-D nozzle, Std. k-ε turbulence model, constant i planes.

(g) Effect of grid size on turbulent energy at x = 100.

Figure 20. – Twelve tab, PAB3D 3-D nozzle solution, 112 grid level.
SZL turbulence model, symmetry plane (j=jmax)

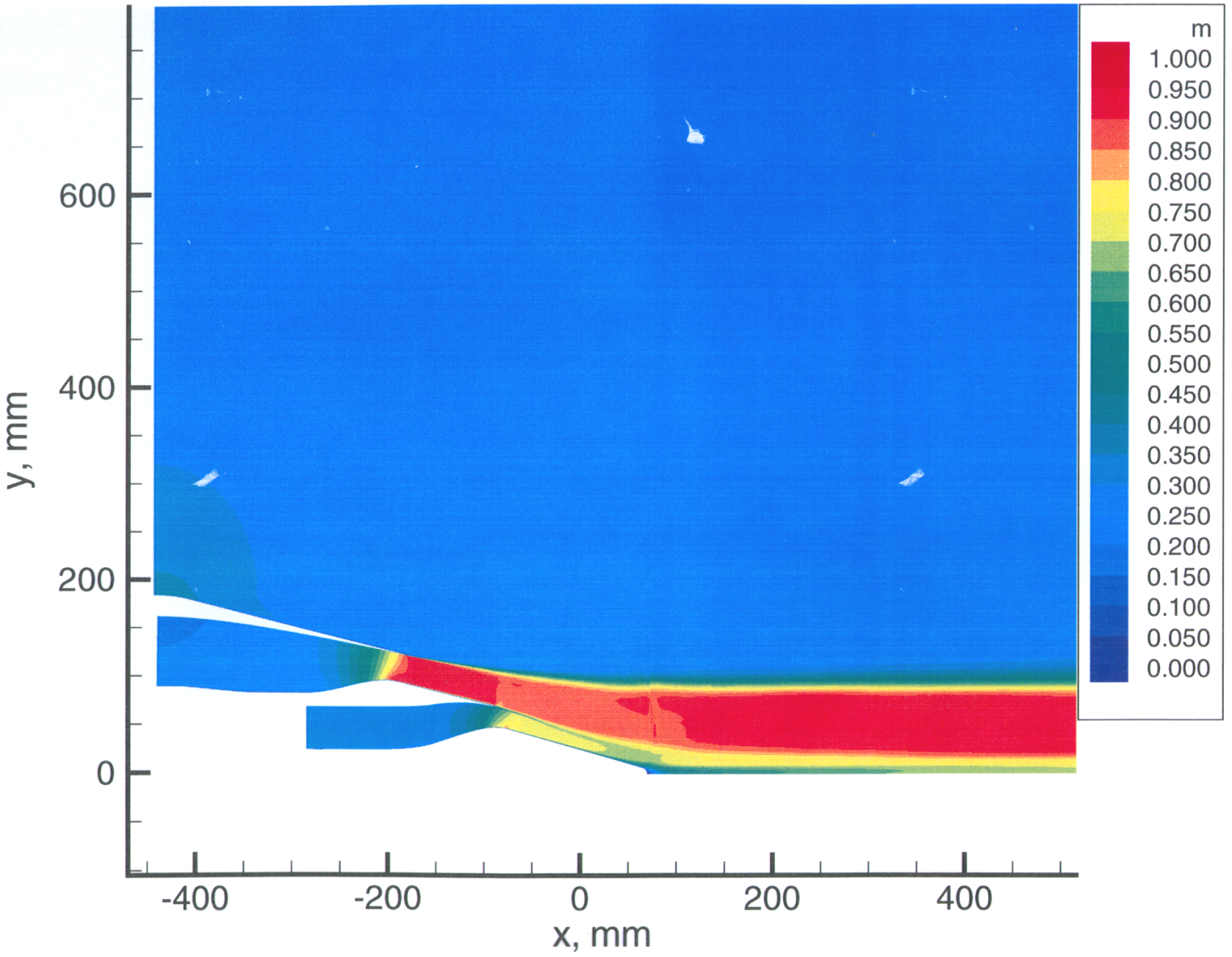

(a) Equal Mach zones in symmetry plane.

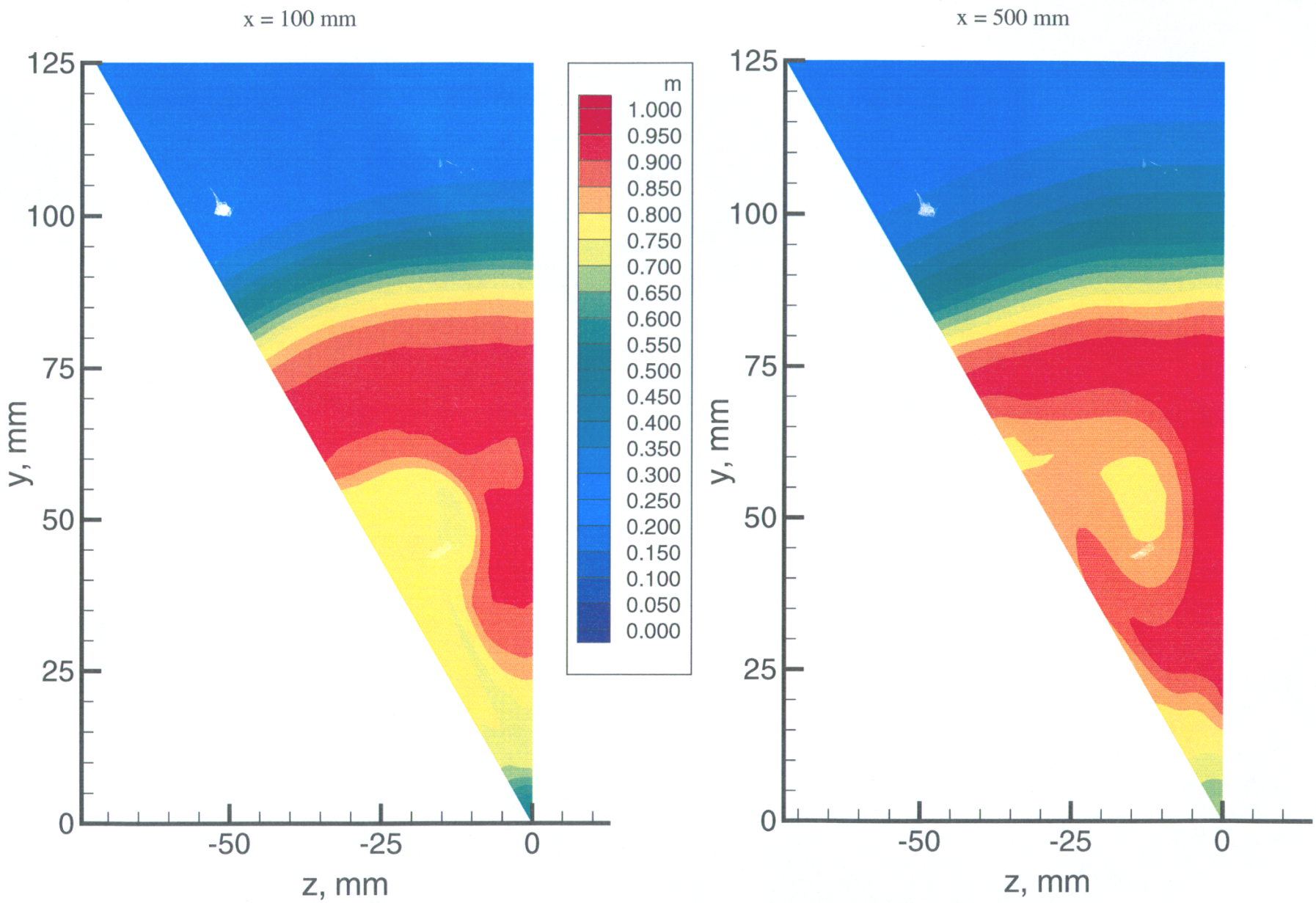

Figure 20. – Twelve tab, PAB3D solution for 3-D nozzle, 112 grid level. SZL turbulence model, constant i planes.

(b) Equal Mach zones at x = 100 and 500 mm.

Figure 20. – Twelve tab, PAB3D 3-D nozzle solution, 112 grid level.
SZL turbulence model, symmetry plane (j=jmax)

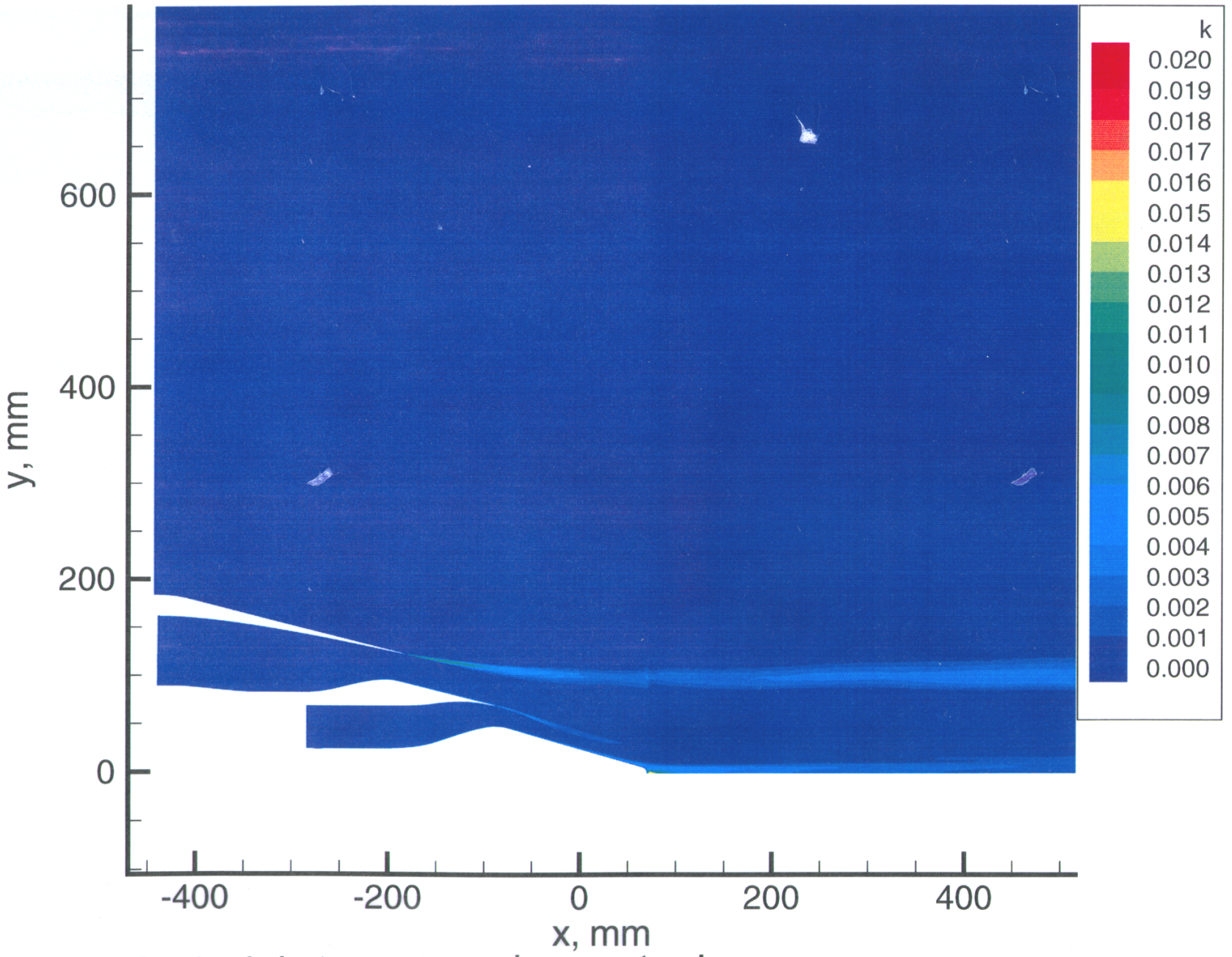

(c) Equal turbulent energy zones in symmetry plane.

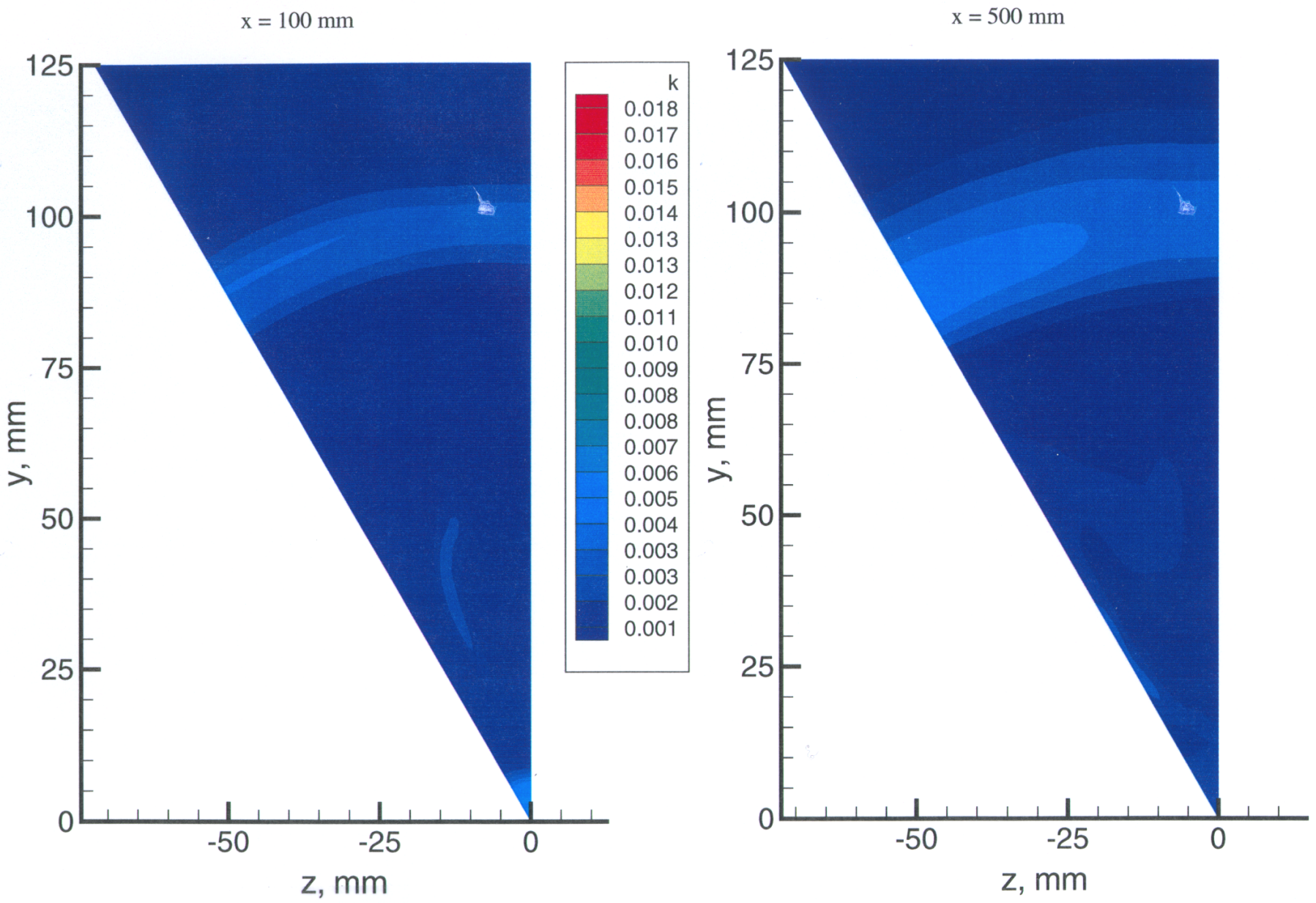

Figure 20. – Twelve tab, PAB3D solution for 3-D nozzle, 112 grid level. SZL turbulence model, constant i planes.

(d) Equal turbulent energy zones at x = 100 and 500 mm.

Figure 20. – Twelve tab, PAB3D 3-D nozzle solution, 112 grid level.
SZL turbulence model, symmetry plane (j=jmax)

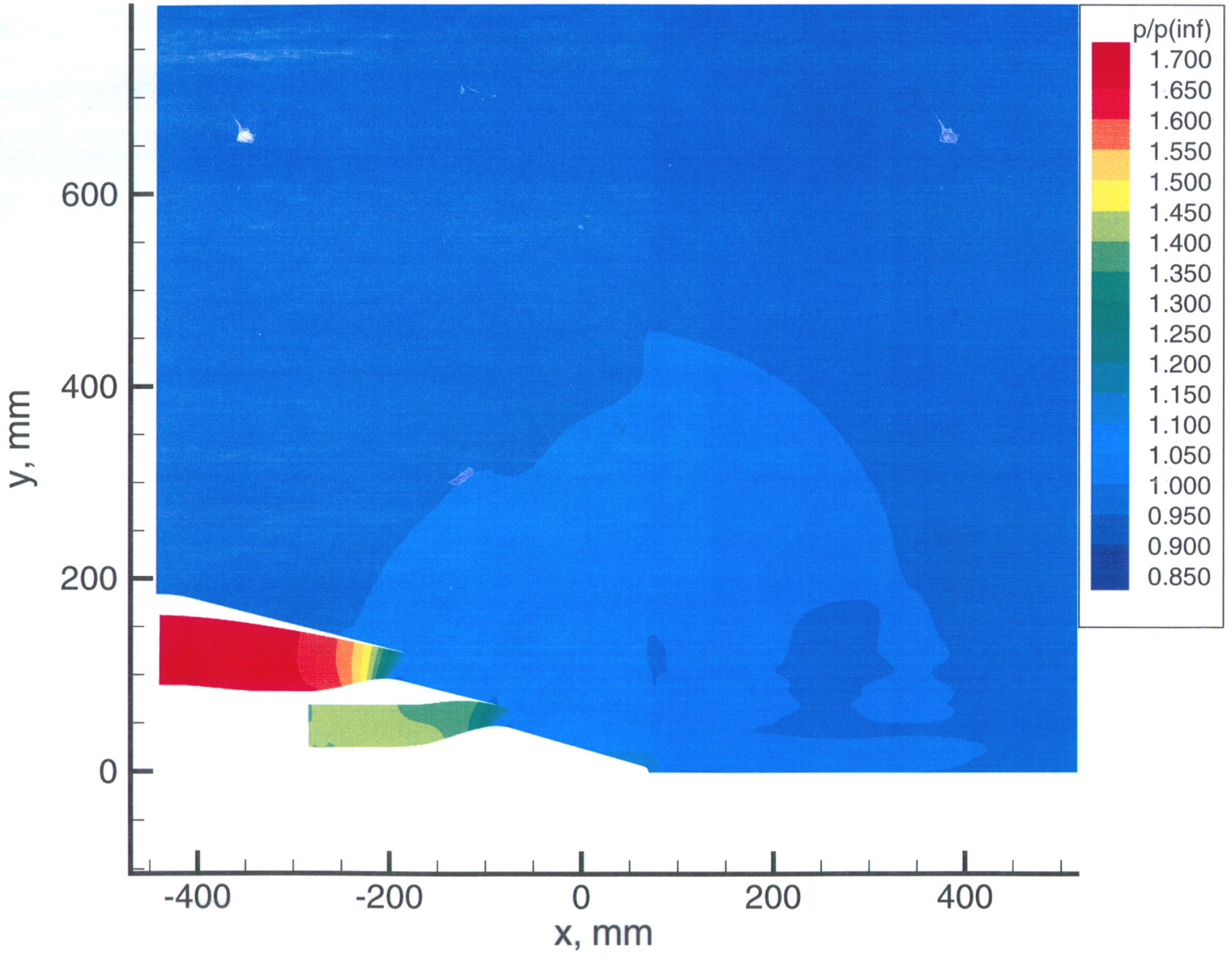

(e) Equal pressure zones in symmetry plane.

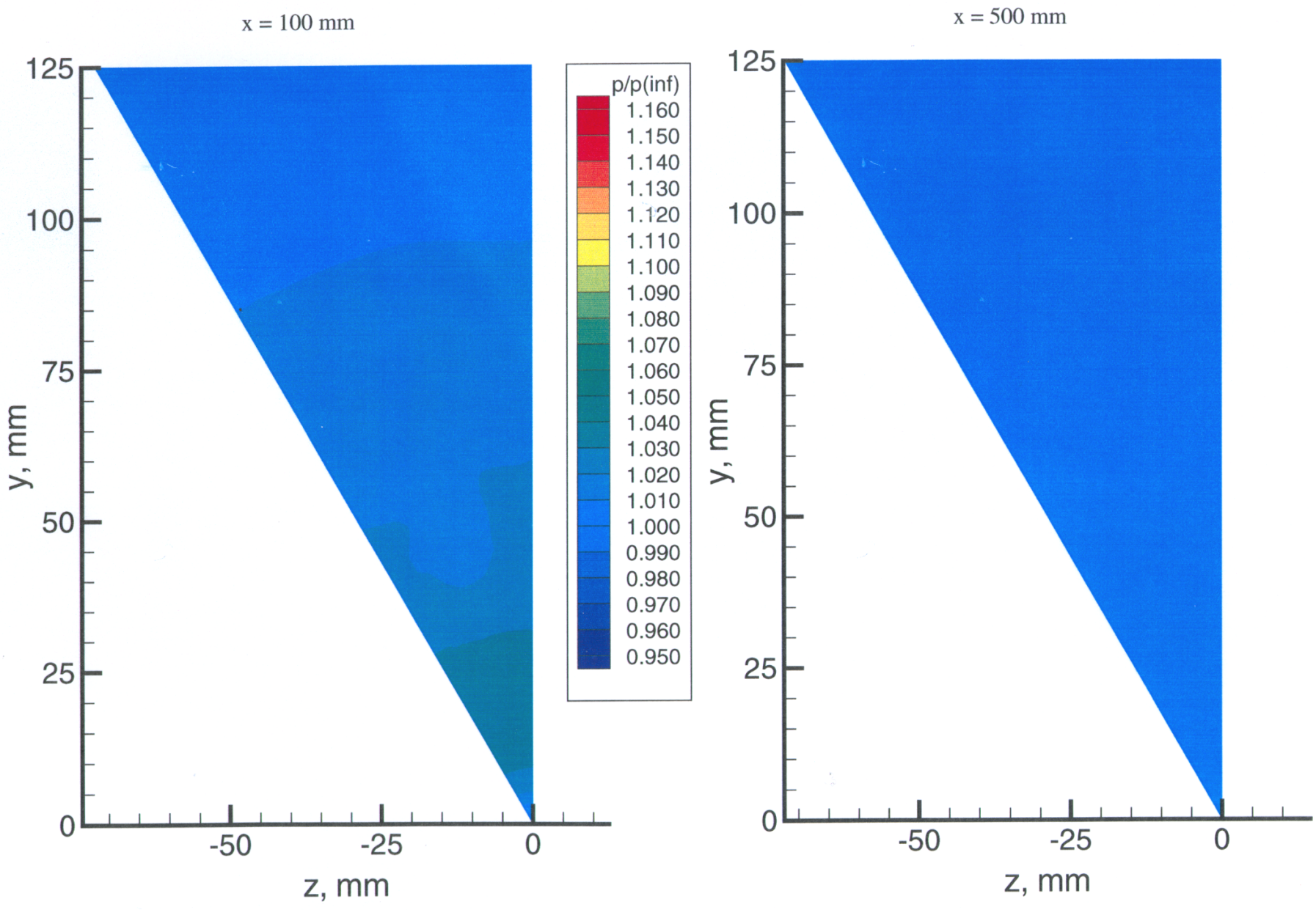

Figure 20. – Twelve tab, PAB3D solution for 3-D nozzle, 112 grid level. SZL turbulence model, constant i planes.

(f) Equal pressure zones at x = 100 and 500 mm.

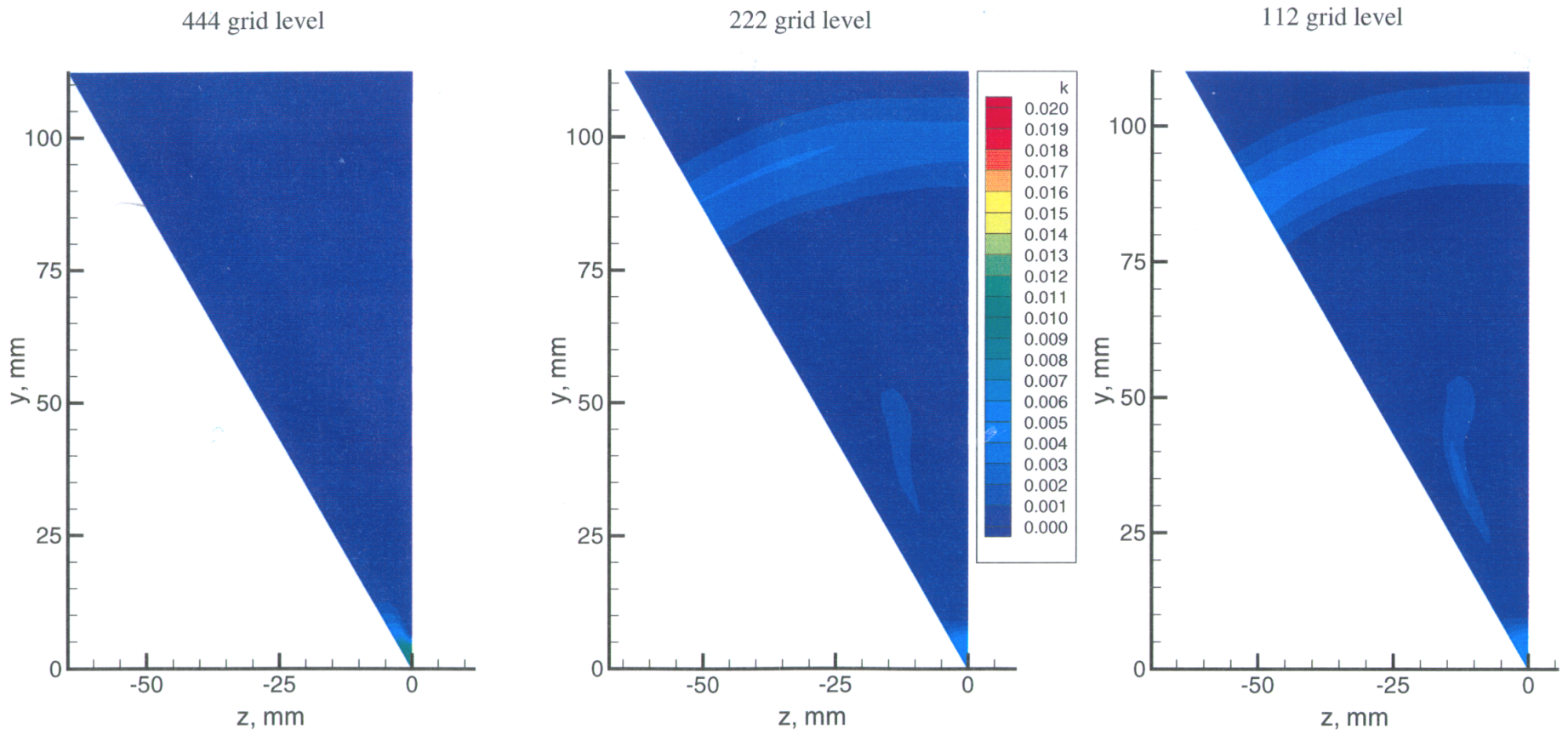

Figure 20. – Twelve tab, PAB3D solution for 3-D nozzle, SZL turbulence model, constant i planes.

(g) Effect of grid size on turbulent energy at x = 100.

Figure 21. – Twenty four tab, 3D configuration,112 grid level.
Std. k-ε turbulence model, symmetry plane (j=jmax)

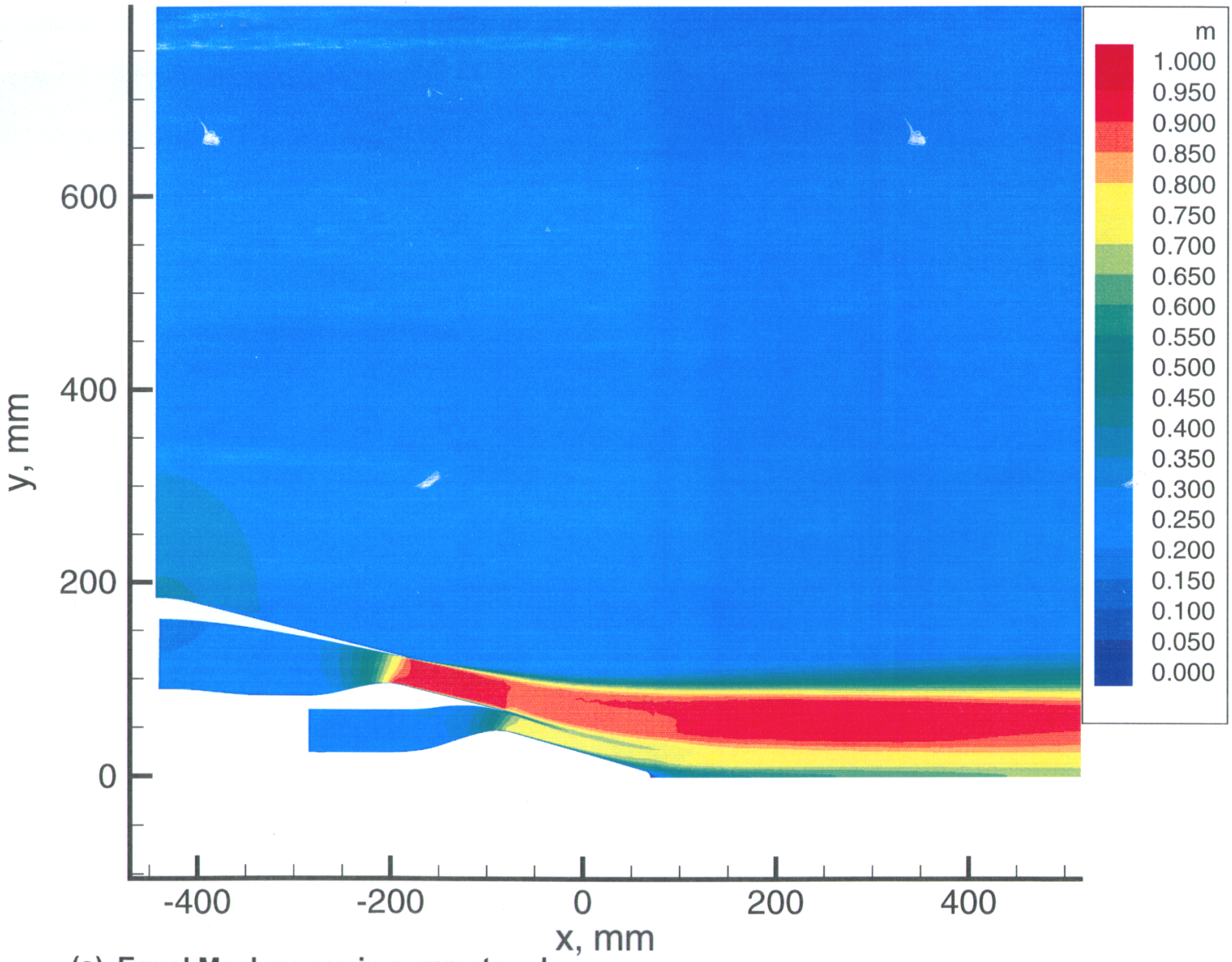

(a) Equal Mach zones in symmetry plane.

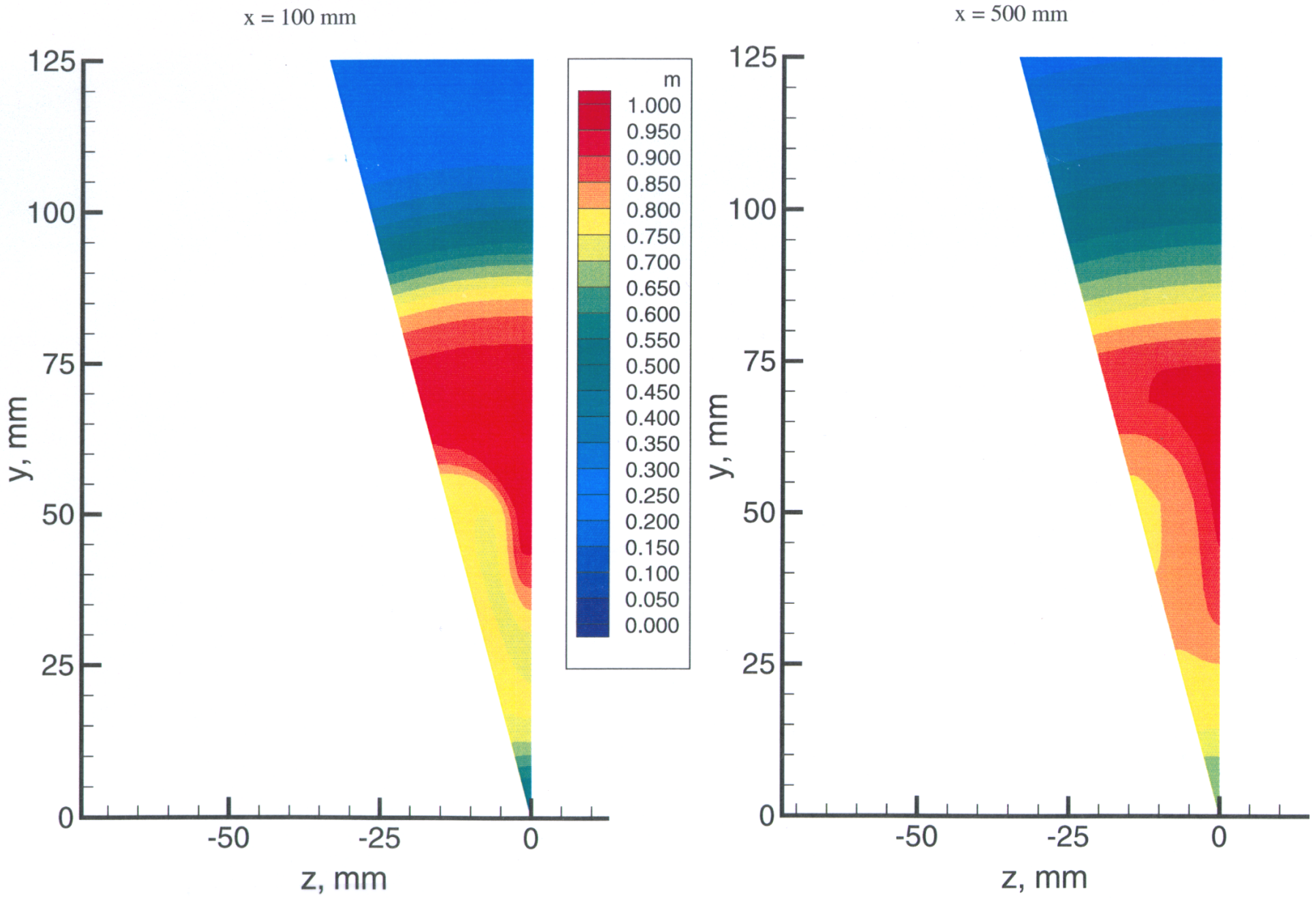

Figure 21. – Twenty four tab, 3D configuration, 112 grid level. Std. k-ϵ turbulence model, constant i planes.

(b) Equal Mach zones at x = 100 and 500 mm.

Figure 21. – Twenty four tab, 3D configuration, 112 grid level.
Std. k-e turbulence model, symmetry plane (j=jmax)

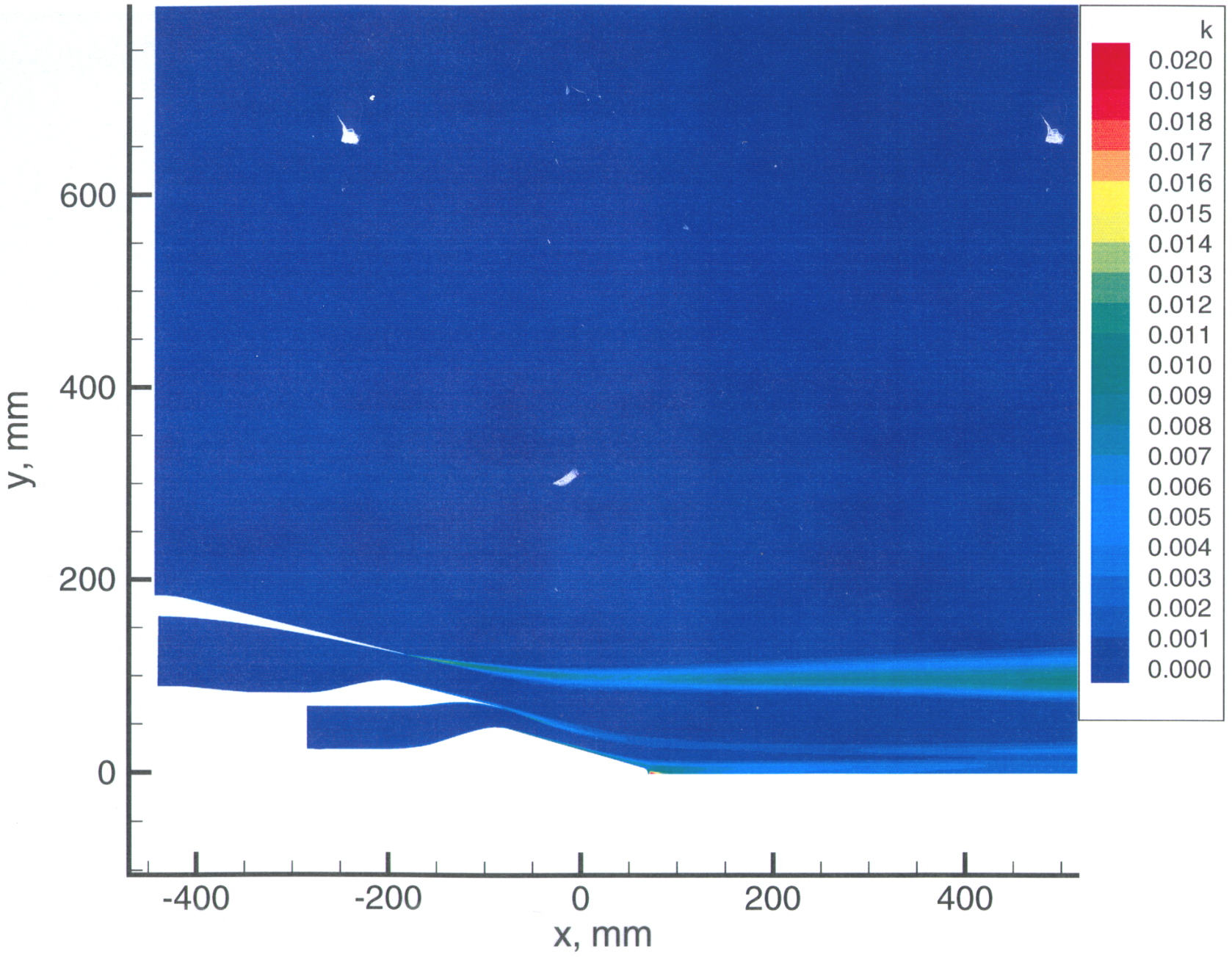

(c) Equal turbulent energy zones in symmetry plane.

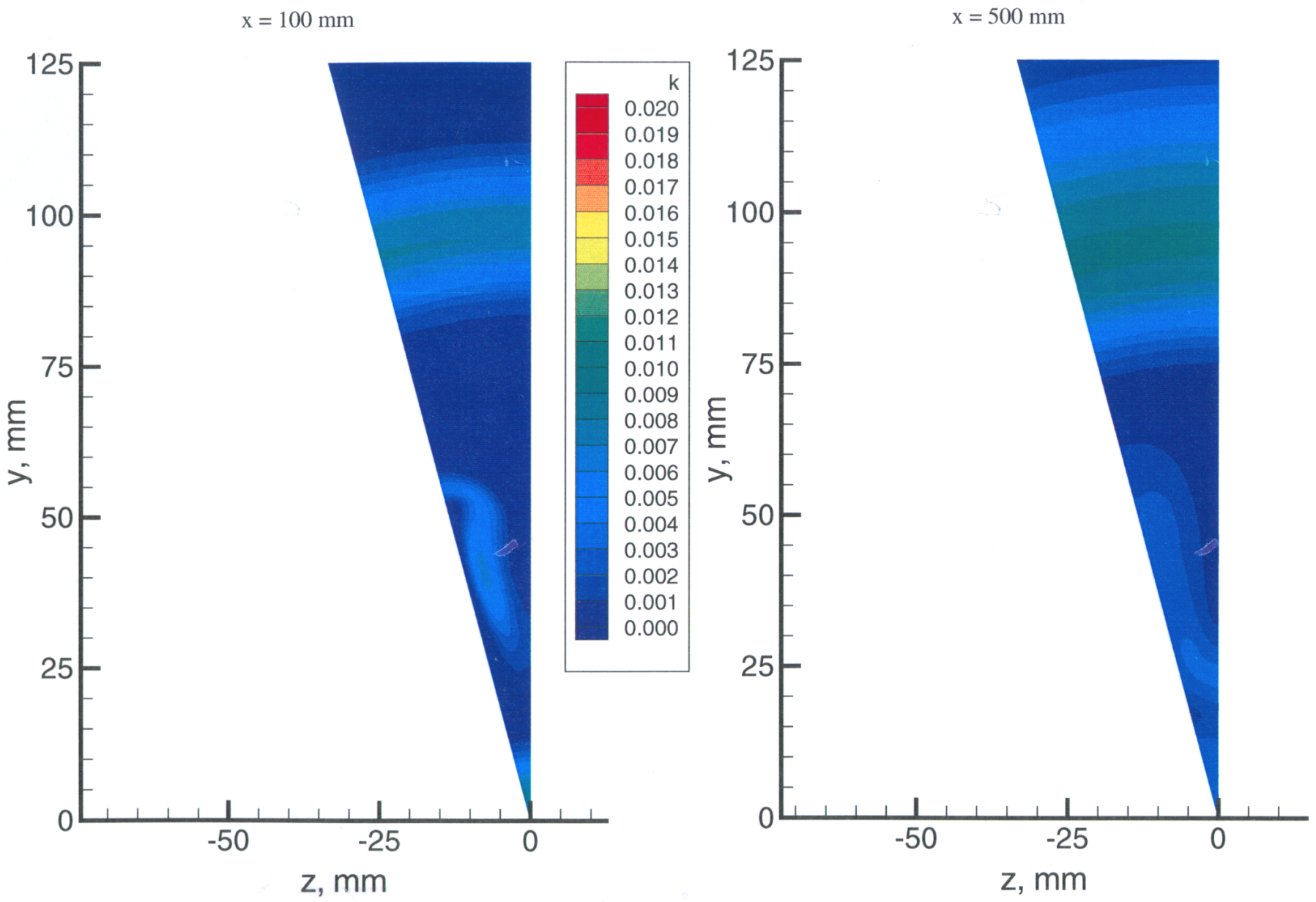

Figure 21. – Twenty four tab, 3D configuration, 112 grid level. Std. k-ϵ turbulence model, constant i planes.

(d) Equal turbulent energy zones at x = 100 and 500 mm.

Figure 21. – Twenty four tab, 3D configuration, 112 grid level.
Std. k-ϵ turbulence model, symmetry plane (j=jmax)

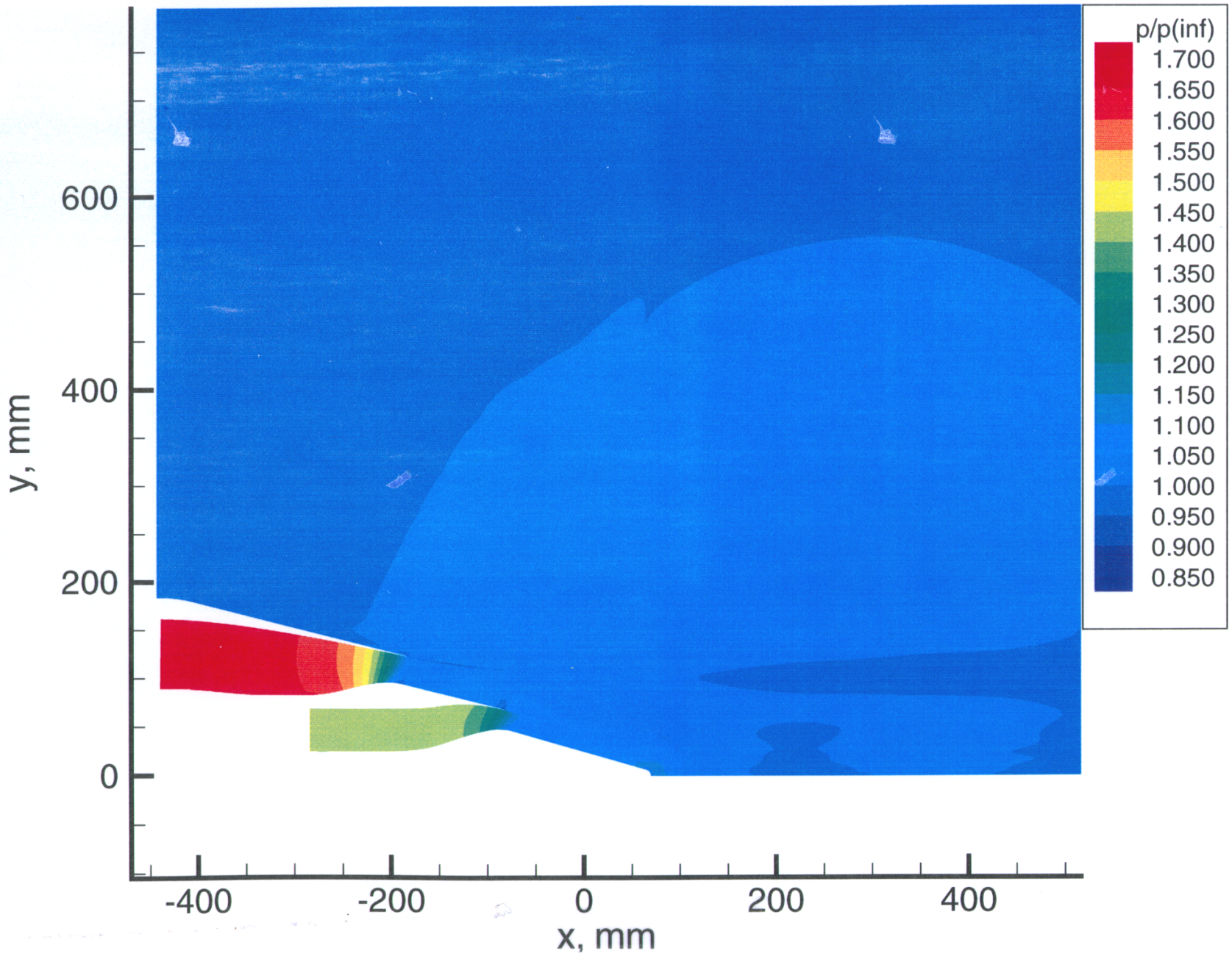

(e) Equal pressure zones in symmetry plane.

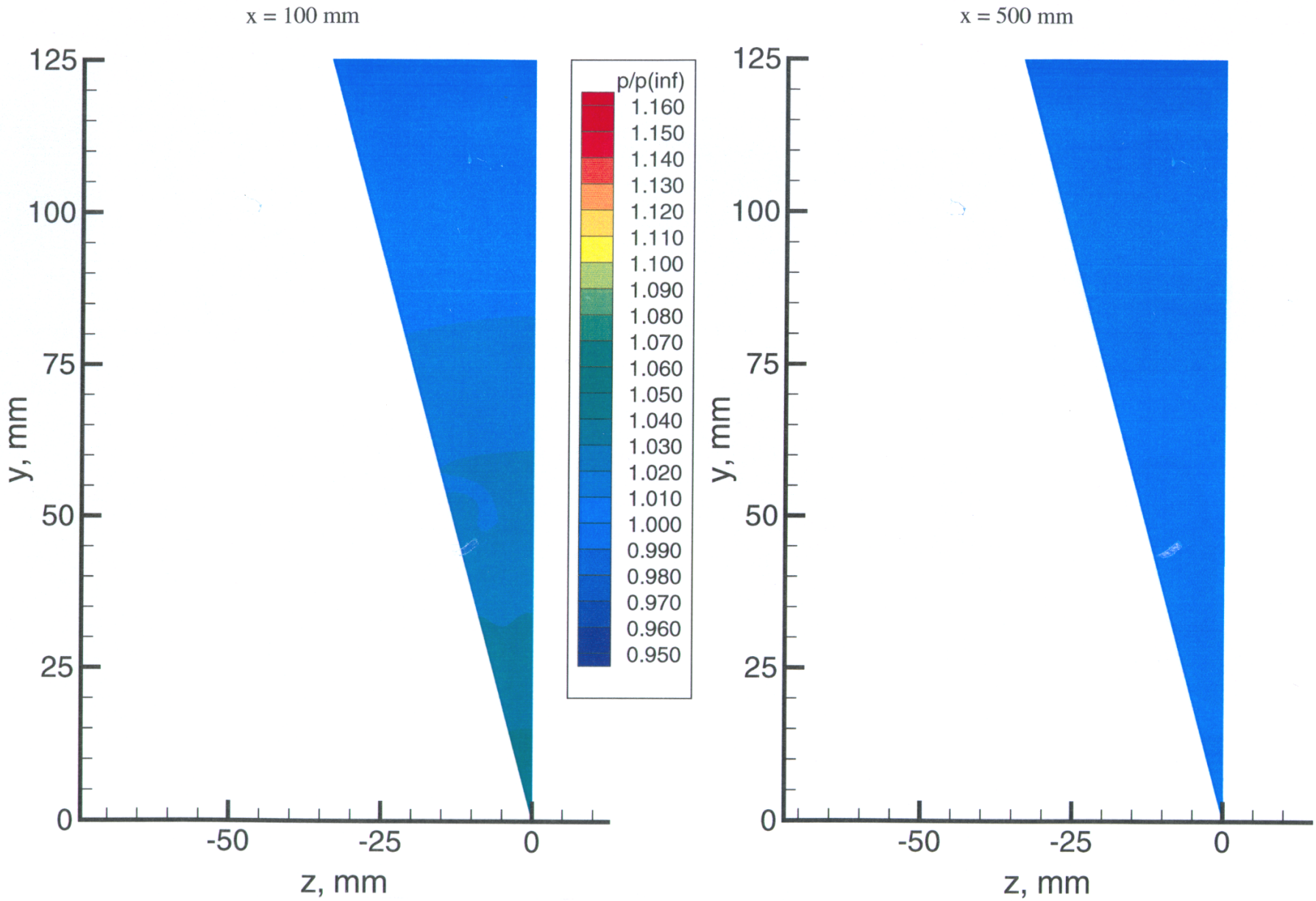

Figure 21. – Twenty four tab, 3D configuration, 112 grid level. Std. k-ϵ turbulence model, constant i planes.

(f) Equal pressure zones at x = 100 and 500 mm.

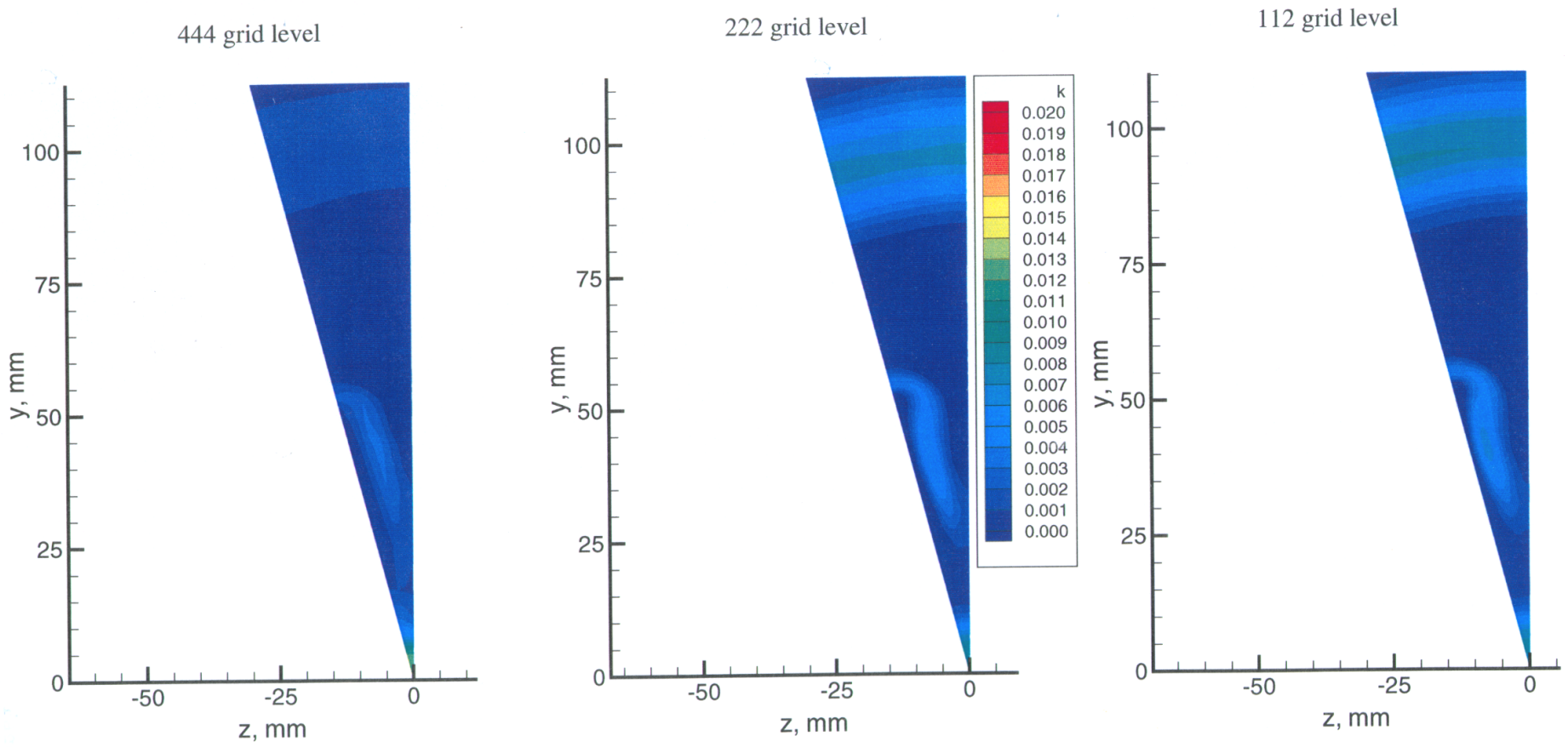

Figure 21. – Twenty four tab, 3D configuration, Std. k-ϵ turbulence model, constant i planes.

(g) Effect of grid size on turbulent energy at x = 100.

REPORT DOCUMENTATION PAGE

Form Approved
OMB No. 0704-0188

Public reporting burden for this collection of information is estimated to average 1 hour per response, including the time for reviewing instructions, searching existing data sources, gathering and maintaining the data needed, and completing and reviewing the collection of information. Send comments regarding this burden estimate or any other aspect of this collection of information, including suggestions for reducing this burden, to Washington Headquarters Services, Directorate for Information Operations and Reports, 1215 Jefferson Davis Highway, Suite 1204, Arlington, VA 22202-4302, and to the Office of Management and Budget, Paperwork Reduction Project (0704-0188), Washington, DC 20503.

1. AGENCY USE ONLY (*Leave blank*)

2. REPORT DATE
May 2001

3. REPORT TYPE AND DATES COVERED
Final Contractor Report

4. TITLE AND SUBTITLE
Jet Plume Flow Solutions

5. FUNDING NUMBERS
WU–781–30–12–00
C73174–5

6. AUTHOR(S)
Percy J. Bobbitt, K.S. Abdol-Hamid, Armin Wulf, and Ana F. Tinetti

7. PERFORMING ORGANIZATION NAME(S) AND ADDRESS(ES)
Eagle Aeronautics, Inc.
12388 Worwick Blvd.
Newport News, Virginia 23606–3850

8. PERFORMING ORGANIZATION REPORT NUMBER
E–12637

9. SPONSORING/MONITORING AGENCY NAME(S) AND ADDRESS(ES)
National Aeronautics and Space Administration
Washington, DC 20546–0001

10. SPONSORING/MONITORING AGENCY REPORT NUMBER
NASA CR—2001-210706

11. SUPPLEMENTARY NOTES
Percy J. Bobbitt and Ana F. Tinetti, Eagle Aeronautics, Inc., 12388 Worwick Blvd., Newport News, Virginia 23606–3850; K.S. Abdol-Hamid, Analytical Services and Materials, Inc., Hampton, Virginia; Armin Wulf, ICEM CFD Engineering, Inc., Berkeley, California. Project Manager, Naseem Saiyed, Structures and Acoustics Division, NASA Glenn Research Center, organization code 5940, 216–433–6736.

12a. DISTRIBUTION/AVAILABILITY STATEMENT
Unclassified - Unlimited
Subject Category: 71 Distribution: Nonstandard
Available electronically at http://gltrs.grc.nasa.gov/GLTRS
This publication is available from the NASA Center for AeroSpace Information, 301–621–0390.

12b. DISTRIBUTION CODE

13. ABSTRACT ***(Maximum 200 words)***
Navier-Stokes CFD solutions of the flow in, and downstream of three plug-nozzle, jet-exhaust configurations are presented. One configuration is axysymmetric, while the other two have “mixing elements” that require three-dimensional grids and flow solutions. Two different turbulence models are used, along with several different combinations of core-nozzle and fan pressure ratios and temperatures to yield a total of six separate flow solutions and associated electronic files. Some illustrative results are presented of Mach number, turbulent kinetic energy, pressure ratio, and the effect of grid size.

14. SUBJECT TERMS
Acoustic nozzles; Aeroacoustics; Aircraft noise; Engine noise; Exhaust nozzles; Jet aircraft noise; Jet engines; Mixers; Noise reduction; Noise suppressors; Sonic nozzles

15. NUMBER OF PAGES
61

16. PRICE CODE

17. SECURITY CLASSIFICATION OF REPORT
Unclassified

18. SECURITY CLASSIFICATION OF THIS PAGE
Unclassified

19. SECURITY CLASSIFICATION OF ABSTRACT
Unclassified

20. LIMITATION OF ABSTRACT